Adaptive control of a DDMR with a Robotic Arm

Rishabh S. Chaure

Thesis submitted to the Faculty of the
Virginia Polytechnic Institute and State University
in partial fulfillment of the requirements for the degree of

Master of Science
in
Mechanical Engineering

Andrea L'Afflitto, Chair
Corina Sandu
Saied Taheri

November 4, 2021
Blacksburg, Virginia

Keywords: Robots, DDMR, wheeled robots, robotic arm, adaptive control

Adaptive control of a DDMR with a Robotic Arm

Rishabh S. Chaure

(ABSTRACT)

Robotic arms are essential in a variety of industrial processes. However, the dexterous workspace of a robotic arm is limited. This limitation can be overcome by making the robotic arm mobile. Such robots, which comprise a robotic manipulator installed on a wheeled mobile platform, are called *mobile robots*. A mobile manipulator can attain a position in space which a robotic arm with fixed base may not be able to reach otherwise. To be applicable to a variety of scenarios, these robots need to meet user-defined margins on their trajectory tracking error, irrespective of the payload transported, faults, and failures. In this thesis, we study the dynamics of mobile manipulator comprising both a differential-drive mobile robot (DDMR) and a robotic arm. Thus, we design a model reference adaptive controller (MRAC) for this mobile manipulator to regulate this vehicle and guarantee robustness to uncertainties in the robot's inertial properties such as the mass of the payload transported and friction coefficients.

Adaptive control of a DDMR with a Robotic Arm

Rishabh S. Chaure

(GENERAL AUDIENCE ABSTRACT)

Humans are able to perform tasks effectively owing to their extraordinary sense of perception and due to their ability to easily grasp things. Although humans are well-suited to perform any process, within an industrial context, a variety of tasks might pose danger to humans, like dealing with hazardous materials or working in extreme environments. Moreover, humans may suffer from fatigue while performing repetitive tasks. These considerations gave rise to the idea of robots which could do the work for humans and instead of humans. Mobile manipulators are a kind of robot that is well-suited for performing a variety of tasks such as collecting, manipulating, and deploying objects from multiple locations. In order to make robots perform a user-specified task, we need to study how the robot reacts to external forces. This knowledge helps us derive a mathematical model for the robotic system. This dynamical model would then be essential in controlling the motion of the robot. In this thesis, we study the dynamics of a mobile manipulator, which comprises a two-wheeled ground platform and a five degrees-of-freedom robotic arm. The dynamical model of this mobile robot is then employed to design a controller that guarantees user-defined margins of error despite uncertainties in some properties, such as the mass of the payload transported.

Acknowledgments

I would like to take this opportunity to express my gratitude to my advisor and mentor, Dr. Andrea L'Afflitto, for giving me this extraordinary opportunity of working under his supervision and carrying out research. Thank you for believing in me that I was capable of learning and carrying out the tasks given to me. I owe my rising interest in the field of robotics and controls, my improvement, and grasp on these topics to Dr. L'Afflitto. Secondly, I would like to thank Dr. Corina Sandu for the course of Modeling and simulation of Multibody dynamics and also for serving as a committee member in my MS committee. I would also like to thank Dr. Saied Taheri for the course of Vehicle control and accepting to serve on my MS committee. I would like to express my gratitude to Adwait Verulkar and Casper Gliech for helping me in my project of the TurtleBot. I would also like to thank Julius Marshall for his invaluable suggestions and clearing my doubts about the programming part.

Contents

List of Figures

List of Tables

List of Abbreviations

DDMR Differential-Drive Mobile Robot

MRAC Model Reference Adaptive Control

$\mathcal{L}$ Lagrangian function

X_A, Y_A coordinates of the center, A, of the track of robot in the inertial reference frame

q vector of the generalized coordinates

r radius of the wheels

w Distance between center of axle to the wheels

x_A, y_A coordinates of the center, A, of the track of robot in the Robot reference frame

α_L angular displacement of the left wheel

α_R angular displacement of the right wheel

θ pitch angle

ϕ roll angle

ψ yaw angle

$\mathbb{O}_{k\times l}$ Zero matrix in $\mathbb{R}^{k\times l}$

$\mathbb{1}_k$ Identity matrix in $\mathbb{R}^{k\times k}$

Chapter 1

Introduction

Automation is the manifestation of the idea to reduce human involvement in processes or tasks, which ultimately gave birth to the idea of machines performing these tasks instead of humans. The first instance of robots being used instead of humans was in the industries. Robots were thought to replace only the repetitive, tedious and injury-prone jobs [1]. Now, robots have been used for a broad spectrum of applications. In industrial setting or construction sites, it is true that we do not need to and we even can not replace humans with robots in each and every aspect, but some tasks, such as transporting objects from a location to another, can definitely be performed without human intervention. Additional examples of tasks in which autonomous mobile robots may replace humans include detecting explosives, removing radioactive wastes and nuclear fuel pellets, exploring other planets or natural satellites, hazardous environments or the seabed, or checking patients affected by an unknown virus. If we need robots to perform human-like tasks then the robots need to be able to think and act intelligently. This establishes the need to study the robots and design control algorithms able to execute complex tasks autonomously.

In this thesis, we study the dynamical model of a decoupled system of mobile manipulators, that is, a five-link robotic arm installed on a differential-drive mobile robot (DDMR), such as the one shown in Figure 1.1 and obtained by merging a TurtleBot3 DDMR and a WidowX200 robotic arm. In particular, we derive its equations of motion, and design adaptive controllers to make the mobile manipulator follow a desired trajectory, assuming that

the effects coupling the DDMR's and the robotic arm's dynamics are negligible.

This thesis is structured as follows. Chapter 2 discusses the literature related to different dynamical models of wheeled robots and robotic manipulators, and the various control techniques employed to perform user-specific tasks. Chapter 3 explains the dynamics of DDMRs for planar and non-planar motion and ultimately derives its equations of motion. Chapter 4 presents a model reference adaptive control (MRAC) architecture to regulate a DDMR. Chapter 5 solves the forward and inverse kinematic problems of a 5 degrees-of-freedom (DOF) robotic arm, and presents its equations of motion. Chapter 6 deals with the design of MRAC for the robotic arm. Chapter 7 shows the results of numerical simulations and experiments performed on a DDMR equipped with a robotic arm. Finally, Chapter 8 summarizes the main results produced in this thesis and provides future research recommendations.

Figure 1.1: The mobile manipulator

Chapter 2

Literature review

In this thesis, we survey part of the literature related to the dynamics and control of wheeled mobile robots. In particular, we discuss the different control techniques employed to maneuver wheeled mobile robots and perform user-specified tasks. This is followed by a literature review of the dynamics and control of different robotic arms, and mobile manipulators.

2.1 Dynamics and Control of DDMRs

As discussed in [2], in general, there are two types of wheeled ground robots, namely two-wheeled and four-wheeled robots. Two-wheeled mobile robots, referred as *Hilare-type* robots, are driven by two independent motors, while four-wheeled or car-like robots have a single actuator to distribute torque to rear wheels with the help of a differential. The Hilare-type robots often posses a supporting ball for balance or an unactuated caster wheel. For these vehicles, the wheels do not have a steering mechanism and rely on their differential mechanism to turn. Hence, these robots are usually referred as DDMR. This mechanism enables such robots to negotiate a zero-radius turn. The DDMRs are widely used for indoor applications due to the ease of controlling hem by regulating the torque exerted by the wheels.

The kinematic models of the DDMRs considered in most of the literature assume no

slipping at the wheels. Dhaouadi and Hatab [3] derived the dynamical model of a DDMR based on non-holonomic constraints using the Lagrangian method as well as the Newton-Euler methodology, and the equations of motion are expressed in terms of the torques inputs and the angular velocities of the wheels. The authors in Dhaouadi and Hatab [3], however, do not discuss any particular control technique. The DDMR is an under-actuated mechanical system, and hence, the problem of designing the control is not straightforward due to the inherent nonlinearities characterizing a DDMR's dynamics. Fan et al. [4] focus on the problem of trajectory tracking for DDMRs. They observe that proportional-integral-derivative (PID) controllers are not sufficiently robust to achieve desired tracking, and design a backstepping controller. Awatef and Mouna [5] present an inverse dynamic control strategy to address the nonlinearity in the dynamical models of DDMRs. In order to address the nonlinear and nonholonomic properties, Mallem et al. [6] propose a sliding mode approach to achieve asymptotical convergence of states along with a PID-governed internal loop and demonstrate the effectiveness of their approach in simulations.

A key problem in the design of control algorithms for DDMRs for applications of practical interest is the ability to overcome parametric uncertainties, that is, uncertainties in the coefficients that characterize the vehicle's dynamics. In [7], a differentiable and time-varying controller is designed to regulate the matched disturbances in the kinematic model of the DDMR based on the non-holonomic constraint of pure rolling and non-slipping. In particular, a robust tracking controller was designed to achieve globally uniformly ultimately bounded tracking error. Successively, the control inputs were mapped to the linear and angular DDMR velocities. Elferik and Imran [8] designed an adaptive controller based on an Immersion and Invariance framework for controlling the linear and angular velocities of the DDMR.

The design of controller for DDMRs taking into account the wheel slips in the dynami-

cal model is an active research area. Tian and Sarkar [9] designed sharp turning of DDMRs with the introduction of wheel slips through traction forces. In this work, the wheel slip was considered to be small, so that the traction forces could be taken as linear functions of slips. It was further assumed that tire dynamics was faster than DDMR dynamics to model the respective control law. However, in general, the relation between traction forces and slips depends on many other factors like the tire dimensions and materials, thread patterns, camber angle, wheel temperature, surface friction etc. [10] which makes it difficult to formulate the traction forces. The Pacejka model [11] or the Magic Formula was employed in [9] to model traction forces as a function of the slip angle and slip ratios with the assumption that slip information is available. However, the lateral slip is not a function of the wheel angular velocity, thus, rendering the DDMR unactuated in the lateral direction. In order to address this problem, the lateral traction force was taken such that it can be controlled indirectly by regulating the longitudinal traction forces, which in turn are controlled via the wheel torques. Based on an Anti-lock Braking system methodology [12] to maximize the longitudinal traction forces to control wheel slips, a sliding mode-based extremum seeking control technique was employed that maximizes the lateral traction force so that the turn radius is minimized.

2.2 Dynamics and Control of Robotic Arms

The dynamics of multi-link robotic arms depends on the types of joints which connect its links. The Denavit-Hartenberg convention [13] is usually employed to establish reference frames at each joint of an n-link robotic arm. These reference frames are conveniently placed to facilitate the derivation of the forward and inverse kinematics for these mechanical systems, and hence, to deduce their equations of motion. There is a wide range of control

techniques to make the robotic arm follow a user-specified trajectory, some of which are discussed in [2]. Spong et al. [13] introduce inverse dynamics based robust and adaptive control algorithms, which account for parametric uncertainties in the robotic arm's dynamical model. In order to address joint friction and other parametric uncertainties, Ajwad et al. [14] propose a sliding mode control for a 6 DOF robotic arm, and compare PID controller. Li et al. [15] propose employ particle swarm optimization to regulate multi-link robotic arms.

2.3 Dynamics and Control of Mobile Manipulators

The study of mobile manipulators is relatively newer than the study of autonomous ground vehicles and robotic arms, since only recently the miniaturization of electronic devices, such as single-board computers, has allowed merging these two classes of mechanical systems. For this reason, the literature of autonomous mobile robots is relatively less explored. The problem of path planning is emphasized in most of the literature. In general, dynamical models of mobile manipulators can be deduced by considering the ground platform's and the robotic arm's dynamics either as coupled or as decoupled. Belda and Rovný [16] consider a decoupled dynamical model for a system comprising of a 5 DOF robotic arm and a 4-wheeled skid steered mobile robot, and introduce the predictive control design concept for motion control. Alternatively, a coupled system of mobile manipulator was employed by Cholewinski and Mazur [17]. However, in this work, control law is divided into a kinematic controller to generate reference velocity signals and a dynamic controller to enforce the mobile manipulator follow these reference signals. Wu et al. [18] demonstrated the effectiveness of an adaptive sliding mode control to track the desired output trajectory for a coupled system of DDMR and a two-link manipulator. Li et al. [19] devised an output feedback controller for a system of under-actuated mobile manipulator where an observer

was set to estimate the states of the system. Mathew and Jisha [20] employed feedback linearization to design torque-based control law. Chi-wu and Ke-fei [21] applied a robust compensator to a three-link arm on a platform system and achieved trajectory tracking with proportinal-derivative feedback.

Chapter 3

Dynamics of Differential-Drive Mobile Robots

This chapter deals with DDMR and the derivation of the equations of motion. These equations form the base to design the adaptive controller to make the DDMR track a user-specified trajectory. This chapter is divided into Section 3.1 where we discuss the dynamics of DDMR in planar scenario and Section 3.2 where non-planar dynamics are discussed. In each of these sections, the frames of reference and the coordinate transformation are defined, then the constraint-based kinematic formulation is explained and the equations of motion of the DDMR are derived using the kinematic constraints.

3.1 Dynamics of DDMR: Planar case

3.1.1 Reference frames and the transformation matrix

The position and the orientation of the DDMR is represented in two coordinate systems, namely an inertial reference frame and a body reference frame. The inertial frame is denoted by $\mathbb{I} \triangleq \{O; X, Y, Z\}$, where $X, Y, Z \in \mathbb{R}^3$, $\|X\| = \|Y\| = \|Z\| = 1$, $X^{\times}Y = Z$, and Z is aligned with the gravitational force so that the weight of the vehicle is given by $F_g = mgZ$, where $m > 0$ denotes the mass of the DDMR and $g > 0$ denotes the gravitational

acceleration [22]. The body reference frame is denoted by $\mathbb{J}(\cdot) \triangleq \{A(\cdot); x(\cdot), y(\cdot), z(\cdot)\}$, where $x, y, z : [0, \infty) \to \mathbb{R}^3$, $\|x(t)\| = \|y(t)\| = \|z(t)\| = 1$, and $x^{\times}(t)y(t) = z(t)$. In this thesis, we assume that a reference frame fixed on the surface of the Earth is inertial. Although this assumption is incorrect, since the Earth rotates about its axis and around the Sun, the error made by considering an Earth fixed reference frame as inertial is insignificant considering the low speed of the robots [22]. Indeed, the robots addressed in this work are characterized by translational velocities in the order of tens of meters per second or less. The DDMR has two wheels, one on each side and the yaw rate of the robot depends on the angular velocities of the wheels. If the DDMR rotates, then it is convenient to describe its orientation about the center of the axle, A. The position of A is denoted by (X_A, Y_A) in the reference frame $\mathbb{I}$, and (x_A, y_A) in the reference frame $\mathbb{J}(\cdot)$. The yaw angle is defined as [23]

$$\psi(t) \triangleq \begin{cases} \tan^{-1}\left(\frac{\dot{Y}_A(t)}{\dot{X}_A(t)}\right), & \dot{X}_A(t) \geq 0, \\ \pi + \tan^{-1}\left(\frac{\dot{Y}_A(t)}{\dot{X}_A(t)}\right), & \dot{Y}_A(t) \geq 0, \dot{X}_A(t) < 0, \\ -\pi + \tan^{-1}\left(\frac{\dot{Y}_A(t)}{\dot{X}_A(t)}\right), & \dot{Y}_A(t) < 0, \dot{X}_A(t) < 0, \\ +\frac{\pi}{2}, & \dot{Y}_A(t) > 0, \dot{X}_A(t) = 0, \\ -\frac{\pi}{2}, & \dot{Y}_A(t) < 0, \dot{X}_A(t) = 0, \\ \text{undefined}, & \dot{Y}_A(t) = 0, \dot{X}_A(t) = 0. \end{cases} \tag{3.1}$$

Since the DDMR moves in the plane containing the X and Y axes, in this section, the displacement along the Z axis is neglected. Moreover, it is assumed the DDMR does not rotate about the x and y axes. Thus, the position and the orientation of the DDMR can described by the vector $[X_A(t), Y_A(t), \psi(t)]^{\mathrm{T}}$ in the reference frame $\mathbb{I}$, and $[x_A(t), y_A(t), \psi(t)]^{\mathrm{T}}$ in the reference frame $\mathbb{J}(\cdot)$.

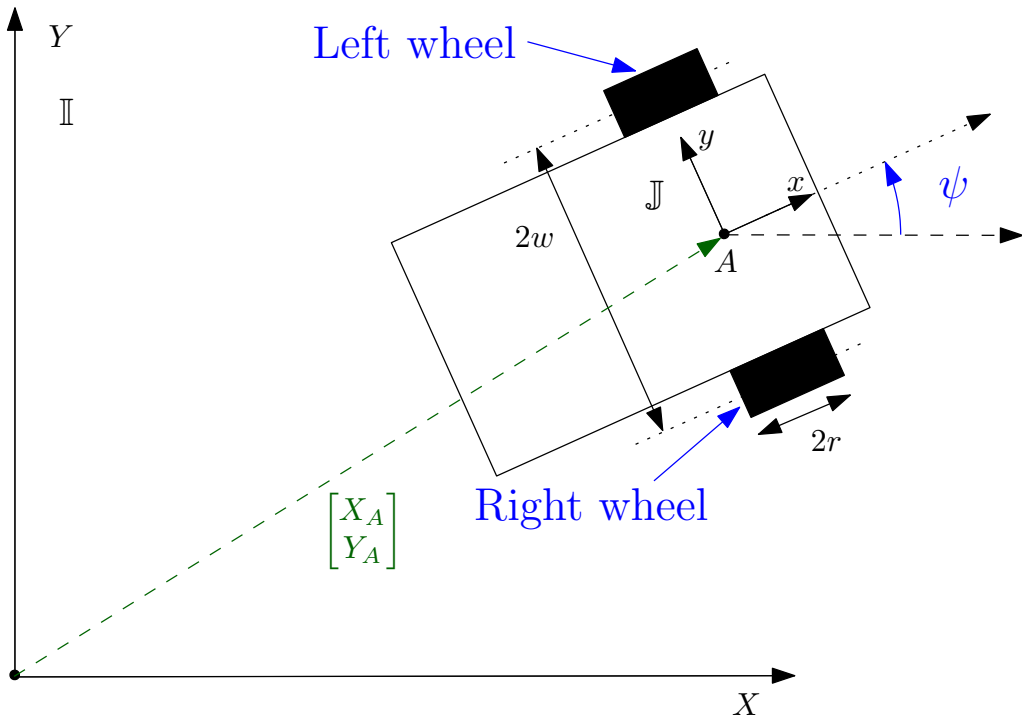

Figure 3.1: Schematic diagram of DDMR: Top view

The DDMR's complete configuration is denoted by the vector of generalized coordinates

$$q \triangleq [X_A \;\; Y_A \;\; \psi \;\; \alpha_R \;\; \alpha_L]^{\mathrm{T}}, \tag{3.2}$$

where $\alpha_{\mathrm{L}}, \alpha_{\mathrm{R}} \in \mathbb{R}$ denote the angular displacement of the left and right wheels, respectively. The rotation matrix that transforms the body reference frame to the inertial frame is

$$\mathbf{R}(\psi) \triangleq \begin{bmatrix} \cos\psi & -\sin\psi & 0 \\ \sin\psi & \cos\psi & 0 \\ 0 & 0 & 1 \end{bmatrix}, \qquad \psi \in [0, 2\pi). \tag{3.3}$$

Since $\mathbf{R}^{\mathrm{T}}(\psi)\mathbf{R}(\psi) = \mathbb{1}_3$, it follows that

$$\dot{\mathbf{R}}^{\mathrm{T}}(\psi(t))\mathbf{R}(\psi(t)) + \mathbf{R}^{\mathrm{T}}(\psi(t))\dot{\mathbf{R}}(\psi(t)) = \mathbb{0}_{3\times 3}, \qquad t \geq 0. \tag{3.4}$$

This implies that $\mathbf{R}^{\mathrm{T}}(\psi(t))\dot{\mathbf{R}}(\psi(t))$ is skew-symmetric for all $t \geq 0$ and hence, we introduce the *angular velocity vector* $\omega : [0, \infty) \to \mathbb{R}^3$ such that $\omega(t) = [\omega_x(t), \omega_y(t), \omega_z(t)]^{\mathrm{T}}$ and

$$\omega^{\times}(t) \triangleq \mathbf{R}^{\mathrm{T}}(\psi(t))\dot{\mathbf{R}}(\psi(t)). \tag{3.5}$$

From (3.3) and (3.5), it follows that

$$\omega^{\times}(t) = \begin{bmatrix} 0 & -\dot{\psi}(t) & 0 \\ \dot{\psi}(t) & 0 & 0 \\ 0 & 0 & 0 \end{bmatrix}, \qquad t \geq 0, \tag{3.6}$$

so that the angular velocity is

$$\omega(t) = [0 \;\; 0 \;\; \dot{\psi}(t)]^{\mathrm{T}}. \tag{3.7}$$

3.1.2 Kinematic constraints

In this thesis, we model the wheels of the DDMR as rigid bodies and the contact between any wheel and the ground is assumed to be at a single point. Also, the wheels are assumed to undergo pure rolling, that is, there is no slipping at the point of contact with the ground; this means the instantaneous velocity of the point of contact is zero. The velocity of the center of right wheel can be computed as

$$V_{\mathrm{rw}}(t) \triangleq \begin{bmatrix} \dot{X}_A(t) \\ \dot{Y}_A(t) \\ 0 \end{bmatrix} + \mathbf{R}(\psi(t)) \left(\omega^{\times}(t) \begin{bmatrix} 0 \\ -w \\ 0 \end{bmatrix} \right), \qquad t \geq 0, \tag{3.8}$$

where $w > 0$ denotes the half width of the axle. Similarly, for the left wheel

$$V_{\mathrm{lw}}(t) \triangleq \begin{bmatrix} \dot{X}_A(t) \\ \dot{Y}_A(t) \\ 0 \end{bmatrix} + \mathbf{R}(\psi(t)) \left(\omega^{\times}(t) \begin{bmatrix} 0 \\ w \\ 0 \end{bmatrix} \right), \qquad t \geq 0. \tag{3.9}$$

The velocity of the point on the right wheel instantaneously in contact with the ground can be computed as

$$V_{\mathrm{rc}}(t) \triangleq V_{\mathrm{rw}}(t) + \mathbf{R}(\psi(t)) \left(\left(\omega(t) + \begin{bmatrix} 0 & \dot{\alpha}_R(t) & 0 \end{bmatrix}^{\mathrm{T}} \right)^{\times} \begin{bmatrix} 0 \\ 0 \\ -r \end{bmatrix} \right), \qquad t \geq 0, \tag{3.10}$$

where $r > 0$ denotes the radius of each wheel, and similarly for the left wheel

$$V_{\mathrm{lc}}(t) \triangleq V_{\mathrm{lw}}(t) + \mathbf{R}(\psi(t)) \left(\left(\omega(t) + \begin{bmatrix} 0 & \dot{\alpha}_L(t) & 0 \end{bmatrix}^{\mathrm{T}} \right)^{\times} \begin{bmatrix} 0 \\ 0 \\ -r \end{bmatrix} \right). \tag{3.11}$$

Equating (3.10) and (3.11) to impose a no-slip condition, we deduce the kinematic constraints

$$\dot{X}_A(t) + w\dot{\psi}(t)\cos\psi(t) - r\dot{\alpha}_R(t)\cos\psi(t) = 0, \qquad t \geq 0, \tag{3.12}$$

$$\dot{Y}_A(t) + w\dot{\psi}(t)\sin\psi(t) - r\dot{\alpha}_R(t)\sin\psi(t) = 0, \tag{3.13}$$

$$\dot{X}_A(t) - w\dot{\psi}(t)\cos\psi(t) - r\dot{\alpha}_L(t)\cos\psi(t) = 0, \tag{3.14}$$

$$\dot{Y}_A(t) - w\dot{\psi}(t)\sin\psi(t) - r\dot{\alpha}_L(t)\sin\psi(t) = 0. \tag{3.15}$$

Multiplying (3.12) by $\cos\psi(t)$, $t \geq 0$, and (3.13) by $\sin\psi(t)$ and adding the resulting equations yields

$$\dot{X}_A(t)\cos\psi(t) + \dot{Y}_A(t)\sin\psi(t) + w\dot{\psi}(t) - r\dot{\alpha}_R(t) = 0, \qquad t \geq 0, \tag{3.16}$$

and multiplying (3.14) by $\cos\psi(t)$ and (3.15) by $\sin\psi(t)$ and adding the resulting equations yields

$$\dot{X}_A(t)\cos\psi(t) + \dot{Y}_A(t)\sin\psi(t) - w\dot{\psi}(t) - r\dot{\alpha}_L(t) = 0. \tag{3.17}$$

Multiplying (3.12) by $-\sin\psi(t)$ and (3.13) by $\cos\psi(t)$ and adding the resulting equations yields

$$-\dot{X}_A(t)\sin\psi(t) + \dot{Y}_A(t)\cos\psi(t) = 0, \qquad t \geq 0, \tag{3.18}$$

and similarly multiplying (3.14) by $-\sin\psi(t)$ and (3.15) by $\cos\psi(t)$ and adding the resulting equations yields the same equation as (3.18).

Equations (3.18), (3.16), and (3.17) can be combined in matrix form as

$$A(q(t))\dot{q}(t) = 0, \qquad t \geq 0, \tag{3.19}$$

where

$$A(q) = \begin{bmatrix} -\sin\psi & \cos\psi & 0 & 0 & 0 \\ \cos\psi & \sin\psi & w & -r & 0 \\ \cos\psi & \sin\psi & -w & 0 & -r \end{bmatrix}, \qquad q \in \mathbb{R}^5. \tag{3.20}$$

Constraints of the form (3.19) are called *Pfaffian constraints* [24, Chapter 1] or, equivalently, non-holonomic velocity constraints as they are not integrable. Since $\operatorname{rank} A(q) = 3$, $q \in \mathbb{R}^5$, it is always possible to find a matrix $S(q) \in \mathbb{R}^{5\times 2}$ of rank 2 such that the columns

of $S(q)$ consist of linearly independent vector fields spanning the null space of $A(q)$ or

$$A(q)S(q) = \mathbb{O}_{3\times 2}, \qquad q \in \mathbb{R}^5. \tag{3.21}$$

From (3.19) and (3.21), it follows that $\dot{q}(\cdot)$ can be expressed in terms of a linear combination of the columns of $S(q)$ as

$$\dot{q}(t) = S(q(t))\dot{\eta}(t), \qquad t \geq 0, \tag{3.22}$$

where $\dot{\eta}(t) \in \mathbb{R}^2$ is to be defined.

The kinematics of the robot are derived with respect to the origin $A(\cdot)$ of the reference frame $\mathbb{J}(\cdot)$. The relation between the rotation of each wheel with the translational speed of point $A(\cdot)$ can be considered in following way. If only one wheel spins then the robot will pivot about the other wheel and the speed of $A(\cdot)$ will be half of that of the spinning wheel. So, the speed of $A(\cdot)$ in the reference frame $\mathbb{J}(\cdot)$ when both wheels spin is

$$\dot{x}_A(t) = \frac{r\dot{\alpha}_R(t) + r\dot{\alpha}_L(t)}{2}, \qquad t \geq 0. \tag{3.23}$$

The DDMR cannot move sideways. Hence,

$$\dot{y}_A(t) = 0, \qquad t \geq 0. \tag{3.24}$$

Now, consider that, if only the right wheel moves forward, then the DDMR will rotate clockwise along the arc of radius equal to the length of its axle, $2w$ and that for only the left wheel spinning, it will rotate counter-clockwise. Thus, the DDMR yaw rate is

$$\dot{\psi}(t) = \frac{r\dot{\alpha}_R(t) - r\dot{\alpha}_L(t)}{2w}, \qquad t \geq 0. \tag{3.25}$$

It follows from (3.23), (3.24), and (3.25) that

$$\begin{bmatrix} \dot{x}_A(t) \\ \dot{y}_A(t) \\ \dot{\psi}(t) \end{bmatrix} = \begin{bmatrix} \frac{r}{2} & \frac{r}{2} \\ 0 & 0 \\ \frac{r}{2w} & -\frac{r}{2w} \end{bmatrix} \begin{bmatrix} \dot{\alpha}_R(t) \\ \dot{\alpha}_L(t) \end{bmatrix}, \qquad t \geq 0. \tag{3.26}$$

Expressing (3.26) in the inertial frame yields

$$\begin{aligned} \begin{bmatrix} \dot{X}_A(t) \\ \dot{Y}_A(t) \\ \dot{\psi}(t) \end{bmatrix} &= \mathbf{R}(\psi(t)) \begin{bmatrix} \dot{x}_A(t) \\ \dot{y}_A(t) \\ \dot{\psi}(t) \end{bmatrix} \\ &= \begin{bmatrix} \cos\psi(t) & -\sin\psi(t) & 0 \\ \sin\psi(t) & \cos\psi(t) & 0 \\ 0 & 0 & 1 \end{bmatrix} \begin{bmatrix} \frac{r}{2} & \frac{r}{2} \\ 0 & 0 \\ \frac{r}{2w} & -\frac{r}{2w} \end{bmatrix} \begin{bmatrix} \dot{\alpha}_R(t) \\ \dot{\alpha}_L(t) \end{bmatrix}, \qquad t \geq 0, \end{aligned} \tag{3.27}$$

or, equivalently,

$$\begin{bmatrix} \dot{X}_A(t) \\ \dot{Y}_A(t) \\ \dot{\psi}(t) \end{bmatrix} = \begin{bmatrix} \frac{r}{2}\cos\psi(t) & \frac{r}{2}\cos\psi(t) \\ \frac{r}{2}\sin\psi(t) & \frac{r}{2}\sin\psi(t) \\ \frac{r}{2w} & -\frac{r}{2w} \end{bmatrix} \begin{bmatrix} \dot{\alpha}_R(t) \\ \dot{\alpha}_L(t) \end{bmatrix}. \tag{3.28}$$

Using (3.2) and (3.28), it holds that

$$\dot{q}(t) = \begin{bmatrix} \frac{r}{2}\cos\psi(t) & \frac{r}{2}\cos\psi(t) \\ \frac{r}{2}\sin\psi(t) & \frac{r}{2}\sin\psi(t) \\ \frac{r}{2w} & -\frac{r}{2w} \\ 1 & 0 \\ 0 & 1 \end{bmatrix} \begin{bmatrix} \dot{\alpha}_R(t) \\ \dot{\alpha}_L(t) \end{bmatrix}, \qquad t \geq 0. \tag{3.29}$$

Comparing (3.29) with (3.22), we deduce that

$$S(q) = \begin{bmatrix} \frac{r}{2}\cos\psi & \frac{r}{2}\cos\psi \\ \frac{r}{2}\sin\psi & \frac{r}{2}\sin\psi \\ \frac{r}{2w} & -\frac{r}{2w} \\ 1 & 0 \\ 0 & 1 \end{bmatrix}, \qquad q \in \mathbb{R}^5, \tag{3.30}$$

and

$$\dot{\eta}(t) = \begin{bmatrix} \dot{\alpha}_R(t) \\ \dot{\alpha}_L(t) \end{bmatrix}, \qquad t \geq 0. \tag{3.31}$$

3.1.3 Equations of Motion of a DDMR

In this thesis, Lagrange's method is used to derive the equations of motion for the DDMR. The *Lagrangian* function for the DDMR is defined as

$$\mathcal{L}(q, \dot{q}) \triangleq T_{\text{total}}(q, \dot{q}) - U_{\text{total}}(q), \qquad (q, \dot{q}) \in \mathbb{R}^5 \times \mathbb{R}^5, \tag{3.32}$$

where $T_{\text{total}} : \mathbb{R}^5 \times \mathbb{R}^5 \to \mathbb{R}$ denotes the *total kinetic energy* and $U_{\text{total}} : \mathbb{R}^5 \to \mathbb{R}$ denotes the *total potential energy* of the DDMR.

For the planar case, the gravitational potential energy is constant, and hence the Lagrangian comprises solely of the kinetic energy term,

$$\mathcal{L}(q, \dot{q}) = T_{\text{total}}(q, \dot{q}), \qquad (q, \dot{q}) \in \mathbb{R}^5 \times \mathbb{R}^5. \tag{3.33}$$

We can write the total kinetic energy of the DDMR as

$$T_{\text{total}}(q,\dot{q}) = T_{\text{b}}(q,\dot{q}) + T_{\text{rw}}(q,\dot{q}) + T_{\text{lw}}(q,\dot{q}), \tag{3.34}$$

where $T_{\text{b}}(\cdot,\cdot)$ denotes the *kinetic energy of the DDMR chassis*, $T_{\text{rw}}(\cdot,\cdot)$ denotes the *kinetic energy of the right wheel*, and $T_{\text{lw}}(\cdot,\cdot)$ denotes the *kinetic energy of the left wheel*. The velocity of the body is given by

$$V_{\text{b}}(t) \triangleq \begin{bmatrix} \dot{X}_A(t) \\ \dot{Y}_A(t) \\ 0 \end{bmatrix} + \mathbf{R}(\psi(t)) \left(\omega^{\times}(t) \begin{bmatrix} x_C \\ y_C \\ z_C \end{bmatrix} \right), \qquad t \geq 0, \tag{3.35}$$

where $[x_C, y_C, z_C]^{\text{T}} \in \mathbb{R}^3$ denotes the position of the center of mass of the platform expressed in the reference frame $\mathbb{J}(\cdot)$. The kinetic energy terms for the chassis, the right wheel, and the left wheel are given by

$$\begin{aligned} T_{\text{b}}(q,\dot{q}) &\triangleq \frac{1}{2} m_{\text{b}} V_{\text{b}}^{\text{T}} V_{\text{b}} + \frac{1}{2} \left(\mathbf{R}(\psi)\omega\right)^{\text{T}} \mathbf{R}(\psi) I_{\text{b}} \mathbf{R}^{\text{T}}(\psi) \left(\mathbf{R}(\psi)\omega\right) \\ &= \frac{1}{2} m_{\text{b}} V_{\text{b}}^{\text{T}} V_{\text{b}} + \frac{1}{2} \omega^{\text{T}} I_{\text{b}} \omega, \qquad (q,\dot{q}) \in \mathbb{R}^5 \times \mathbb{R}^5, \end{aligned} \tag{3.36}$$

$$\begin{aligned} T_{\text{rw}}(q,\dot{q}) &\triangleq \frac{1}{2} m_{\text{w}} V_{\text{rw}}^{\text{T}} V_{\text{rw}} + \frac{1}{2} \left(\mathbf{R}(\psi) \begin{bmatrix} 0 \\ \dot{\alpha}_R \\ \dot{\psi} \end{bmatrix} \right)^{\text{T}} \mathbf{R}(\psi) I_{\text{w}} \mathbf{R}^{\text{T}}(\psi) \left(\mathbf{R}(\psi) \begin{bmatrix} 0 \\ \dot{\alpha}_R \\ \dot{\psi} \end{bmatrix} \right) \\ &= \frac{1}{2} m_{\text{w}} V_{\text{rw}}^{\text{T}} V_{\text{rw}} + \frac{1}{2} \begin{bmatrix} 0 & \dot{\alpha}_R & \dot{\psi} \end{bmatrix} I_{\text{w}} \begin{bmatrix} 0 & \dot{\alpha}_R & \dot{\psi} \end{bmatrix}^{\text{T}}, \end{aligned} \tag{3.37}$$

$$T_{\text{lw}}(q,\dot{q}) \triangleq \frac{1}{2} m_{\text{w}} V_{\text{lw}}^{\text{T}} V_{\text{lw}} + \frac{1}{2} \begin{bmatrix} 0 & \dot{\alpha}_L & \dot{\psi} \end{bmatrix} I_{\text{w}} \begin{bmatrix} 0 & \dot{\alpha}_L & \dot{\psi} \end{bmatrix}^{\text{T}}, \tag{3.38}$$

where $m_{\text{b}} > 0$ denotes the *mass of the DDMR chassis*, $m_{\text{w}} > 0$ denotes the *mass of each wheel*, and $I_{\text{b}} \in \mathbb{R}^{3\times3}$ and $I_{\text{w}} \in \mathbb{R}^{3\times3}$ denote the *moment of inertia matrices for the*

DDMR chassis and the wheels, respectively, expressed in the reference frame $\mathbb{J}(\cdot)$, such that $I_{\mathrm{b}} = \begin{bmatrix} I_{\mathrm{b}_1} & 0 & 0 \\ 0 & I_{\mathrm{b}_2} & 0 \\ 0 & 0 & I_{\mathrm{b}_3} \end{bmatrix}$ and $I_{\mathrm{w}} = \begin{bmatrix} I_{\mathrm{w}_1} & 0 & 0 \\ 0 & I_{\mathrm{w}_2} & 0 \\ 0 & 0 & I_{\mathrm{w}_3} \end{bmatrix}$.

The Lagrange's equations of motion for the DDMR can be written as

$$\frac{d}{dt}\left[\frac{\partial \mathcal{L}(q,\dot{q})}{\partial \dot{q}}\right] - \frac{\partial \mathcal{L}(q,\dot{q})}{\partial q} = A^{\mathrm{T}}(q)\lambda + B(q)\tau, \qquad (q,\dot{q},\lambda) \in \mathbb{R}^5 \times \mathbb{R}^5 \times \mathbb{R}^3, \tag{3.39}$$

where $\lambda \in \mathbb{R}^3$ denotes the *vector of Lagrange multipliers*, $\tau \in \mathbb{R}^2$ denotes the *input vector* comprising of the torques for the wheels of the DDMR, and $B(q) \triangleq \begin{bmatrix} \mathbb{O}_{3\times 2} \\ \mathbb{1}_2 \end{bmatrix}$. The kinetic energy terms (3.36), (3.38), and (3.37) are computed using (3.8), (3.9) , and (3.35) and then finally, we deduce (3.34). Thus, it follows from (3.33) and (3.39) that

$$\begin{aligned} \frac{d}{dt}&\begin{bmatrix} m\dot{X}_A(t) - m_b\dot{\psi}(t)\left(y_C\cos\psi(t) + x_C\sin\psi(t)\right) \\ m\dot{Y}_A(t) + m_b\dot{\psi}(t)(x_C\cos\psi(t) - y_C\sin\psi(t)) \\ I\dot{\psi}(t) - m_b\dot{X}_A(t)(y_C\cos\psi(t) + x_C\sin\psi(t)) + m_b\dot{Y}_A(t)(x_C\cos\psi(t) - y_C\sin\psi(t)) \\ I_{\mathrm{w}}\dot{\alpha}_R(t) \\ I_{\mathrm{w}}\dot{\alpha}_L(t) \end{bmatrix} \\ &= \begin{bmatrix} 0 \\ 0 \\ -\dot{\psi}(t)m_b\dot{X}_A(t)(x_C\cos\psi(t) - y_C\sin\psi(t)) - \dot{\psi}(t)m_b\dot{Y}_A(t)(y_C\cos\psi(t) + x_C\sin\psi(t)) \\ 0 \\ 0 \end{bmatrix} \\ &\quad + A^{\mathrm{T}}(q(t))\lambda + B(q(t))\tau(t), \qquad q(0) = q_0, \qquad \dot{q}(0) = \dot{q}_0, \qquad t \geq 0, \end{aligned} \tag{3.40}$$

where $m \triangleq m_{\mathrm{b}} + 2m_{\mathrm{w}}$ and $I \triangleq I_{b_3} + m_{\mathrm{b}}(x_C^2 + y_C^2) + 2m_{\mathrm{w}}w^2 + 2I_{w_3}$. Equation (3.40) can be written as

$$\begin{aligned} \mathcal{M}(q(t))\ddot{q}(t) + \mathcal{C}(q(t), \dot{q}(t))\dot{q}(t) = A^{\mathrm{T}}(q(t))\lambda + B(q(t))\tau(t), \\ q(0) = q_0, \qquad \dot{q}(0) = \dot{q}_0, \qquad t \geq 0, \end{aligned} \tag{3.41}$$

where (3.42) denotes the generalized mass matrix and (3.41) captures the *centripetal and Coriolis terms*

$$\mathcal{M}(q) \triangleq \begin{bmatrix} m & 0 & M_{13} & 0 & 0 \\ 0 & m & M_{23} & 0 & 0 \\ M_{13} & M_{23} & I & 0 & 0 \\ 0 & 0 & 0 & I_{w_2} & 0 \\ 0 & 0 & 0 & 0 & I_{w_2} \end{bmatrix}, \qquad (q, \dot{q}) \in \mathbb{R}^5 \times \mathbb{R}^5, \tag{3.42}$$

$$\mathcal{C}(q, \dot{q}) \triangleq \begin{bmatrix} 0 & 0 & -\dot{\psi}M_{23} & 0 & 0 \\ 0 & 0 & \dot{\psi}M_{13} & 0 & 0 \\ 0 & 0 & 0 & 0 & 0 \\ 0 & 0 & 0 & 0 & 0 \\ 0 & 0 & 0 & 0 & 0 \end{bmatrix}, \tag{3.43}$$

$M_{13} \triangleq -m_b(y_C \cos\psi + x_C \sin\psi)$, and $M_{23} \triangleq m_b(x_C \cos\psi - y_C \sin\psi)$. Differentiating (3.22) and using (3.30) and (3.31), we deduce that

$$\ddot{q}(t) = S(q(t))\ddot{\eta}(t) + \dot{S}(q(t))\dot{\eta}(t), \qquad t \geq 0. \tag{3.44}$$

Substituting (3.44) in (3.41) and rearranging the resulting equation yields

$$\mathcal{M}(q)S(q)\ddot{\eta} + \mathcal{M}(q)\dot{S}(q)\dot{\eta} + \mathcal{C}(q,\dot{q})S(q)\dot{\eta} = A^{\mathrm{T}}(q)\lambda + B(q)\tau. \tag{3.45}$$

The Lagrange multiplier λ is unknown. In order to eliminate λ from (3.45), we pre-multiply (3.45) by $S^{\mathrm{T}}(q)$ to deduce that

$$\begin{aligned} S^{\mathrm{T}}(q(t))\mathcal{M}(q(t))S(q(t))\ddot{\eta} + [S^{\mathrm{T}}(q(t))\mathcal{M}(q(t))\dot{S}(q(t)) + S^{\mathrm{T}}(q(t))\mathcal{C}(q(t),\dot{q}(t))S(q(t))]\dot{\eta(t)} = \\ S^{\mathrm{T}}(q(t))B(q(t))\tau(t), \qquad q(0) = q_0, \qquad \dot{q}(0) = \dot{q}_0, \\ \eta(0) = [\mathbb{O}_{2\times 6}\ \mathbb{1}_2]q_0, \qquad \dot{\eta}(0) = [\mathbb{O}_{2\times 6}\ \mathbb{1}_2]\dot{q}_0. \end{aligned} \tag{3.46}$$

Now defining

$$\bar{\mathcal{M}}(q) \triangleq S^{\mathrm{T}}(q)\mathcal{M}(q)S(q), \qquad (q,\dot{q}) \in \mathbb{R}^5 \times \mathbb{R}^5, \tag{3.47}$$

$$\bar{\mathcal{C}}(q,\dot{q}) \triangleq S^{\mathrm{T}}(q)\mathcal{M}(q)\dot{S}(q) + S^{\mathrm{T}}(q)\mathcal{C}(q,\dot{q})S(q), \tag{3.48}$$

and noting that $S^{\mathrm{T}}(q)B(q) = \mathbb{1}_2$, (3.46) is reduced to the form

$$\begin{aligned} \bar{\mathcal{M}}(q(t))\ddot{\eta}(t) + \bar{\mathcal{C}}(q(t),\dot{q}(t))\dot{\eta}(t) = \tau(t), \qquad q(0) = q_0, \qquad \dot{q}(0) = \dot{q}_0, \\ \eta(0) = [\mathbb{O}_{2\times 6}\mathbb{1}_2]q_0, \qquad \dot{\eta}(0) = [\mathbb{O}_{2\times 6}\mathbb{1}_2]\dot{q}_0, \end{aligned} \tag{3.49}$$

where

$$\bar{\mathcal{M}}(q) = \begin{bmatrix} I_{w_2} + \frac{r^2}{4w^2}(mw^2 + I) & \frac{r^2}{4w^2}(mw^2 - I) \\ \frac{r^2}{4w^2}(mw^2 - I) & I_{w_2} + \frac{r^2}{4w^2}(mw^2 + I) \end{bmatrix}, \tag{3.50}$$

$$\bar{\mathcal{C}}(q,\dot{q}) = \begin{bmatrix} 0 & \frac{r^2}{2w} m_{\mathrm{b}} x_C \dot{\psi} \\ -\frac{r^2}{2w} m_{\mathrm{b}} x_C \dot{\psi} & 0 \end{bmatrix}. \tag{3.51}$$

3.2 Dynamics of DDMR: Non-planar case

3.2.1 Reference frames and the transformation matrix

In this section, we remove the restriction of planar motion of the DDMR. For this case, the definitions for the inertial frame and the body reference frame of the DDMR remain the same as that for the planar case. Since the motion of the DDMR is not restricted to a plane, we have to consider rolling and pitching of the DDMR as well, which are denoted by $\phi \in [0, 2\pi)$ and $\theta \in \left(-\frac{\pi}{2}, \frac{\pi}{2}\right)$ respectively. The vector of generalized coordinates is defined as

$$q \triangleq [X_A \;\; Y_A \;\; Z_A \;\; \phi \;\; \theta \;\; \psi \;\; \alpha_R \;\; \alpha_L]^{\mathrm{T}}. \tag{3.52}$$

The rotation matrix that transforms the reference frame $\mathbb{J}(\cdot)$ to the inertial frame $\mathbb{I}$ is given by

$$\mathbf{R}(\phi,\theta,\psi) \triangleq \begin{bmatrix} \cos\psi\cos\theta & \cos\psi\sin\phi\sin\theta - \cos\phi\sin\psi & \sin\psi\sin\phi + \cos\psi\cos\phi\sin\theta \\ \cos\theta\sin\psi & \cos\psi\cos\phi + \sin\psi\sin\phi\sin\theta & \cos\phi\sin\psi\sin\theta - \cos\psi\sin\phi \\ -\sin\theta & \cos\theta\sin\phi & \cos\phi\cos\theta \end{bmatrix}, \tag{3.53}$$

$$(\phi,\theta,\psi) \in [0,2\pi) \times \left(-\frac{\pi}{2}, \frac{\pi}{2}\right) \times [0,2\pi).$$

For brevity, we write $\mathbf{R}(\phi, \theta, \psi)$ as

$$\mathbf{R}(\phi, \theta, \psi) = \begin{bmatrix} R_{11} & R_{12} & R_{13} \\ R_{21} & R_{22} & R_{23} \\ R_{31} & R_{32} & R_{33} \end{bmatrix}. \tag{3.54}$$

Since $\mathbf{R}^{\mathrm{T}}(\phi, \theta, \psi)\,\mathbf{R}(\phi, \theta, \psi) = \mathbb{1}_3$, it follows that

$$\begin{aligned} \dot{\mathbf{R}}^{\mathrm{T}}(\phi(t), \theta(t), \psi(t))\,\mathbf{R}(\phi(t), \theta(t), \psi(t)) + \mathbf{R}^{\mathrm{T}}(\phi(t), \theta(t), \psi(t))\,\dot{\mathbf{R}}(\phi(t), \theta(t), \psi(t)) \\ = \mathbb{O}_{3\times 3}, \qquad t \geq 0. \end{aligned} \tag{3.55}$$

This implies that $\mathbf{R}^{\mathrm{T}}(\phi(t), \theta(t), \psi(t))\,\dot{\mathbf{R}}(\phi(t), \theta(t), \psi(t))$ is skew-symmetric for all $t \geq 0$ and hence, we introduce the *angular velocity vector* $\omega : [0, \infty) \to \mathbb{R}^3$ such that $\omega(t) = [\omega_x(t), \omega_y(t), \omega_z(t)]^{\mathrm{T}}$ and

$$\omega^{\times}(t) \triangleq \mathbf{R}^{\mathrm{T}}(\phi(t), \theta(t), \psi(t))\,\dot{\mathbf{R}}(\phi(t), \theta(t), \psi(t)). \tag{3.56}$$

From (3.53) and (3.56), the body angular velocity can be computed as

$$\omega(t) = \begin{bmatrix} \dot{\phi}(t) - \dot{\psi}(t)\sin\theta(t) \\ \dot{\theta}(t)\cos\phi(t) + \dot{\psi}(t)\cos\theta(t)\sin\phi(t) \\ \dot{\psi}(t)\cos\phi(t)\cos\theta(t) - \dot{\theta}(t)\sin\phi(t) \end{bmatrix}, \qquad t \geq 0. \tag{3.57}$$

3.2.2 Kinematic constraints

Similar to the kinematic constraints for the planar case discussed in Section 3.1.2, the wheels are assumed to undergo pure rolling. Hence, the instantaneous velocity at the point of contact between the wheels and the ground is taken to be zero. The velocity of the center

of right wheel can be computed as

$$V_{\mathrm{rw}}(t) \triangleq \begin{bmatrix} \dot{X}_A(t) \\ \dot{Y}_A(t) \\ \dot{Z}_A(t) \end{bmatrix} + \mathbf{R}\left(\phi(t), \theta(t), \psi(t)\right) \left(\omega^{\times}(t) \begin{bmatrix} 0 \\ -w \\ 0 \end{bmatrix} \right), \qquad t \geq 0. \tag{3.58}$$

Similarly, for the left wheel

$$V_{\mathrm{lw}}(t) \triangleq \begin{bmatrix} \dot{X}_A(t) \\ \dot{Y}_A(t) \\ \dot{Z}_A(t) \end{bmatrix} + \mathbf{R}\left(\phi(t), \theta(t), \psi(t)\right) \left(\omega^{\times}(t) \begin{bmatrix} 0 \\ w \\ 0 \end{bmatrix} \right). \tag{3.59}$$

The velocity of the point on the right wheel instantaneously in contact with the ground can be computed as

$$V_{\mathrm{rc}}(t) \triangleq V_{\mathrm{rw}}(t) + \mathbf{R}\left(\phi(t), \theta(t), \psi(t)\right) \left[\left(\omega(t) + \begin{bmatrix} 0 \\ \dot{\alpha}_R(t) \\ 0 \end{bmatrix} \right)^{\times} \begin{bmatrix} 0 \\ 0 \\ -r \end{bmatrix} \right], \qquad t \geq 0, \tag{3.60}$$

where $r > 0$ denotes the radius of each wheel, and similarly for the left wheel

$$V_{\mathrm{lc}}(t) \triangleq V_{\mathrm{lw}}(t) + \mathbf{R}\left(\phi(t), \theta(t), \psi(t)\right) \left[\left(\omega(t) + \begin{bmatrix} 0 \\ \dot{\alpha}_L(t) \\ 0 \end{bmatrix} \right)^{\times} \begin{bmatrix} 0 \\ 0 \\ -r \end{bmatrix} \right]. \tag{3.61}$$

Equating (3.60) and (3.61) to zero, we deduce the kinematic constraint equations and write them in matrix form as

$$A(q(t))\dot{q}(t) = 0, \qquad t \geq 0, \tag{3.62}$$

where

$$A(q) \triangleq \begin{bmatrix} 1 & 0 & 0 & A_{14} & A_{15} & A_{16} & A_{17} & 0 \\ 0 & 1 & 0 & A_{24} & A_{25} & A_{26} & A_{27} & 0 \\ 0 & 0 & 1 & A_{34} & A_{35} & 0 & A_{37} & 0 \\ 1 & 0 & 0 & A_{44} & A_{45} & A_{46} & 0 & A_{17} \\ 0 & 1 & 0 & A_{54} & A_{55} & A_{56} & 0 & A_{27} \\ 0 & 0 & 1 & A_{64} & A_{65} & 0 & 0 & A_{37} \end{bmatrix}, \qquad q \in \mathbb{R}^8, \tag{3.63}$$

$$A_{14} \triangleq R_{31}\left(wR_{22} + rR_{23}\right) - R_{21}\left(wR_{32} + rR_{33}\right), \tag{3.64}$$

$$A_{15} \triangleq -wR_{32}\cos\psi - rR_{33}\cos\psi, \tag{3.65}$$

$$A_{16} \triangleq wR_{22} + rR_{23}, \tag{3.66}$$

$$A_{17} \triangleq r(R_{23}R_{32} - R_{22}R_{33}), \tag{3.67}$$

$$A_{24} \triangleq -R_{31}\left(wR_{12} + rR_{13}\right) + R_{11}\left(wR_{32} + rR_{33}\right), \tag{3.68}$$

$$A_{25} \triangleq -wR_{32}\sin\psi - rR_{33}\sin\psi, \tag{3.69}$$

$$A_{26} \triangleq -wR_{12} - rR_{13}, \tag{3.70}$$

$$A_{27} \triangleq r(R_{12}R_{33} - R_{13}R_{32}), \tag{3.71}$$

$$A_{34} \triangleq R_{21}\left(wR_{12} + rR_{13}\right) - R_{11}\left(wR_{22} + rR_{23}\right), \tag{3.72}$$

$$A_{35} \triangleq \cos\psi\left(wR_{12} + rR_{13}\right) + \sin\psi\left(wR_{22} + rR_{23}\right), \tag{3.73}$$

$$A_{37} \triangleq r(R_{13}R_{22} - R_{12}R_{23}), \tag{3.74}$$

$$A_{44} \triangleq -R_{31}\left(wR_{22} - rR_{23}\right) + R_{21}\left(wR_{32} - rR_{33}\right), \tag{3.75}$$

$$A_{45} \triangleq wR_{32}\cos\psi - rR_{33}\cos\psi, \tag{3.76}$$

$$A_{46} \triangleq -wR_{22} + rR_{23}, \tag{3.77}$$

$$A_{54} \triangleq -R_{31}\left(-wR_{12} + rR_{13}\right) + R_{11}\left(-wR_{32} + rR_{33}\right), \tag{3.78}$$

$$A_{55} \triangleq wR_{32}\sin\psi - rR_{33}\sin\psi, \tag{3.79}$$

$$A_{56} \triangleq wR_{12} - rR_{13}, \tag{3.80}$$

$$A_{64} \triangleq R_{21}\left(-wR_{12} + rR_{13}\right) - R_{11}\left(-wR_{22} + rR_{23}\right), \tag{3.81}$$

$$A_{65} \triangleq \cos\psi\left(-wR_{12} + rR_{13}\right) + \sin\psi\left(-wR_{22} + rR_{23}\right). \tag{3.82}$$

It is assumed that the DDMR does not lose contact with the ground for all $t \geq 0$. Hence,

$$\dot{z}_A(t) = 0, \qquad t \geq 0. \tag{3.83}$$

From (3.23), (3.24), (3.83), and (3.31), it follows that

$$\begin{bmatrix} \dot{x}_A(t) \\ \dot{y}_A(t) \\ \dot{z}_A(t) \end{bmatrix} = \begin{bmatrix} \frac{r}{2} & \frac{r}{2} \\ 0 & 0 \\ 0 & 0 \end{bmatrix} \dot{\eta}(t), \qquad t \geq 0. \tag{3.84}$$

Expressing (3.84) in the inertial frame yields

$$\begin{bmatrix} \dot{X}_A(t) \\ \dot{Y}_A(t) \\ \dot{Z}_A(t) \end{bmatrix} = \mathbf{R}\left(\phi(t), \theta(t), \psi(t)\right) \begin{bmatrix} \dot{x}_A(t) \\ \dot{y}_A(t) \\ \dot{z}_A(t) \end{bmatrix}, \tag{3.85}$$

or, equivalently,

$$\begin{bmatrix} \dot{X}_A(t) \\ \dot{Y}_A(t) \\ \dot{Z}_A(t) \end{bmatrix} = \begin{bmatrix} \frac{r}{2}\cos\psi(t)\cos\theta(t) & \frac{r}{2}\cos\psi(t)\cos\theta(t) \\ \frac{r}{2}\sin\psi(t)\cos\theta(t) & \frac{r}{2}\sin\psi(t)\cos\theta(t) \\ -\frac{r}{2}\sin\theta(t) & -\frac{r}{2}\sin\theta(t) \end{bmatrix} \dot{\eta}(t), \qquad t \geq 0. \tag{3.86}$$

Since we assume that the DDMR and its tyres are modeled as rigid bodies, the DDMR can not rotate about the x and y axes of the body reference frame. Hence, we can express the

body angular velocity $\omega(\cdot)$ using (3.25) as

$$\omega(t) = \begin{bmatrix} 0 \\ 0 \\ \frac{r}{2w}\left(\dot{\alpha}_R(t) - \dot{\alpha}_L(t)\right) \end{bmatrix}, \qquad t \geq 0. \tag{3.87}$$

Comparing (3.87) with (3.57) and solving for the the angular velocities yields

$$\begin{bmatrix} \dot{\phi}(t) \\ \dot{\theta}(t) \\ \dot{\psi}(t) \end{bmatrix} = \begin{bmatrix} \frac{r}{2w}\cos\phi(t)\tan\theta(t) & -\frac{r}{2w}\cos\phi(t)\tan\theta(t) \\ -\frac{r}{2w}\sin\phi(t) & \frac{r}{2w}\sin\phi(t) \\ \frac{r}{2w}\cos\phi(t)\cos\theta(t) & -\frac{r}{2w}\cos\phi(t)\cos\theta(t) \end{bmatrix} \dot{\eta}(t), \qquad t \geq 0. \tag{3.88}$$

Thus, from (3.86) and (3.88) we can deduce that

$$\dot{q}(t) = S(q(t))\dot{\eta}(t), \qquad t \geq 0, \tag{3.89}$$

where

$$S(q) \triangleq \begin{bmatrix} \frac{r}{2}\cos\psi\cos\theta & \frac{r}{2}\cos\psi\cos\theta \\ \frac{r}{2}\sin\psi\cos\theta & \frac{r}{2}\sin\psi\cos\theta \\ -\frac{r}{2}\sin\theta & -\frac{r}{2}\sin\theta \\ \frac{r}{2w}\cos\phi\tan\theta & -\frac{r}{2w}\cos\phi\tan\theta \\ -\frac{r}{2w}\sin\phi & \frac{r}{2w}\sin\phi \\ \frac{r}{2w}\cos\phi\cos\theta & -\frac{r}{2w}\cos\phi\cos\theta \\ 1 & 0 \\ 0 & 1 \end{bmatrix}, \qquad q \in \mathbb{R}^8. \tag{3.90}$$

It can be verified from (3.63) and (3.90) that

$$A(q)S(q) = \mathbb{O}_{6\times 2}, \qquad q \in \mathbb{R}^8. \tag{3.91}$$

3.2.3 Equations of Motion

The *Lagrangian* function for the DDMR is given by

$$\mathcal{L}(q,\dot{q}) = T_{\text{total}}(q,\dot{q}) - U_{\text{total}}(q), \qquad (q,\dot{q}) \in \mathbb{R}^8 \times \mathbb{R}^8, \tag{3.92}$$

where $T_{\text{total}} : \mathbb{R}^8 \times \mathbb{R}^8 \to \mathbb{R}$ denotes the *total kinetic energy* and $U_{\text{total}} : \mathbb{R}^8 \to \mathbb{R}$ denotes the *total potential energy* of the DDMR. The total kinetic energy of the DDMR is same as that in (3.34). Now, the velocity of the chassis is given by

$$V_{\text{b}}(t) = \begin{bmatrix} \dot{X}_A(t) \\ \dot{Y}_A(t) \\ \dot{Z}_A(t) \end{bmatrix} + \mathbf{R}\left(\phi(t),\theta(t),\psi(t)\right) \left(\omega^{\times}(t) \begin{bmatrix} x_C \\ y_C \\ z_C \end{bmatrix} \right), \qquad t \geq 0. \tag{3.93}$$

where $[x_C, y_C, z_C]^{\text{T}} \in \mathbb{R}^3$ denotes the position of the center of mass of the platform defined in the reference frame $\mathbb{J}(\cdot)$. The kinetic energy terms for the chassis, the right wheel, and the left wheel are given by

$$T_{\text{b}}(q,\dot{q}) = \frac{1}{2} m_{\text{b}} V_{\text{b}}^{\text{T}} V_{\text{b}} + \frac{1}{2} \omega^{\text{T}} I_{\text{b}}\, \omega, \qquad (q,\dot{q}) \in \mathbb{R}^8 \times \mathbb{R}^8, \tag{3.94}$$

$$T_{\text{rw}}(q,\dot{q}) = \frac{1}{2} m_{\text{w}} V_{\text{rw}}^{\text{T}} V_{\text{rw}} + \frac{1}{2} \left(\omega + \begin{bmatrix} 0 \\ \dot{\alpha}_R \\ 0 \end{bmatrix} \right)^{\text{T}} I_{\text{w}} \left(\omega + \begin{bmatrix} 0 \\ \dot{\alpha}_R \\ 0 \end{bmatrix} \right), \tag{3.95}$$

$$T_{\text{lw}}(q,\dot{q}) = \frac{1}{2} m_{\text{w}} V_{\text{lw}}^{\text{T}} V_{\text{lw}} + \frac{1}{2} \left(\omega + \begin{bmatrix} 0 \\ \dot{\alpha}_L \\ 0 \end{bmatrix} \right)^{\text{T}} I_{\text{w}} \left(\omega + \begin{bmatrix} 0 \\ \dot{\alpha}_L \\ 0 \end{bmatrix} \right), \tag{3.96}$$

respectively, where $m_{\mathrm{b}} > 0$ denotes the *mass of the DDMR chassis*, $m_{\mathrm{w}} > 0$ denotes the *mass of the wheel*, and $I_{\mathrm{b}} \in \mathbb{R}^{3\times3}$ and $I_{\mathrm{w}} \in \mathbb{R}^{3\times3}$ denote the moment of inertia matrices for the DDMR chassis and the wheels, respectively, expressed in the reference frame $\mathbb{J}(\cdot)$. The total potential energy of the DDMR is computed as

$$U_{\mathrm{total}}(q) = m_{\mathrm{b}} g(Z_A + R_{31}x_C + R_{32}y_C + R_{33}z_C) + 2m_{\mathrm{w}} g Z_A, \qquad q \in \mathbb{R}^8. \tag{3.97}$$

The Lagrange's equations of motion for the DDMR for the non-planar case can be written as

$$\frac{d}{dt}\left[\frac{\partial \mathcal{L}(q,\dot{q})}{\partial \dot{q}}\right] - \frac{\partial \mathcal{L}(q,\dot{q})}{\partial q} = A^{\mathrm{T}}(q)\lambda + B(q)\tau, \qquad (q,\dot{q},\lambda) \in \mathbb{R}^8 \times \mathbb{R}^8 \times \mathbb{R}^6, \tag{3.98}$$

where $\lambda \in \mathbb{R}^6$ denotes the vector of Lagrange multipliers, $\tau \in \mathbb{R}^2$ is the input vector comprising of torques for the wheels of the DDMR, and $B(q) = \begin{bmatrix} \mathbb{O}_{6\times2} \\ \mathbb{1}_2 \end{bmatrix}$. Simplifying and rearranging (3.98), we can write

$$\mathcal{M}(q)\ddot{q} + \mathcal{C}(q,\dot{q})\dot{q} + \mathcal{K}(q) = A^{\mathrm{T}}(q)\lambda + B(q)\tau, \qquad (q,\dot{q},\lambda,\tau) \in \mathbb{R}^8 \times \mathbb{R}^8 \times \mathbb{R}^6 \times \mathbb{R}^2, \tag{3.99}$$

where $\mathcal{M}(q)$ denotes the *generalized mass matrix*, $\mathcal{C}(q,\dot{q})$ denotes the *centripetal and Coriolis matrix* and $\mathcal{K}(q)$ denotes the *generalized gravitational force*; the expressions for $\mathcal{M}(\cdot)$, $\mathcal{C}(\cdot,\cdot)$, and $\mathcal{K}(\cdot)$ are omitted for brevity.

As already discussed in Section 3.1.3, in order to eliminate the unknown λ from (3.99),

we pre-multiply (3.99) by $S^{\mathrm{T}}(q)$ and substituting (3.44) in the resulting equation yields

$$\begin{aligned} S^{\mathrm{T}}(q(t))\mathcal{M}(q(t))S(q(t))\ddot{\eta} + [S^{\mathrm{T}}(q(t))\mathcal{M}(q(t))\dot{S}(q(t)) + S^{\mathrm{T}}(q(t))\mathcal{C}(q(t),\dot{q}(t))S(q(t))]\dot{\eta} \\ +S^{\mathrm{T}}(q(t))\mathcal{K}(q(t)) = S^{\mathrm{T}}(q(t))B(q(t))\tau(t), \qquad q(0) = q_0, \qquad \dot{q}(0) = \dot{q}_0, \\ \eta(0) = [\mathbb{O}_{2\times 6}\mathbb{1}_2]q_0, \qquad \dot{\eta}(0) = [\mathbb{O}_{2\times 6}\mathbb{1}_2]\dot{q}_0. \end{aligned} \tag{3.100}$$

where $\eta \triangleq [\alpha_R \quad \alpha_L]^{\mathrm{T}}$. Now, defining

$$\bar{\mathcal{M}}(q) = S^{\mathrm{T}}(q)\mathcal{M}(q)S(q), \qquad (q,\dot{q}) \in \mathbb{R}^8 \times \mathbb{R}^8, \tag{3.101}$$

$$\bar{\mathcal{C}}(q,\dot{q}) = S^{\mathrm{T}}(q)\mathcal{M}(q)\dot{S}(q) + S^{\mathrm{T}}(q)\mathcal{C}(q,\dot{q})S(q), \tag{3.102}$$

$$\bar{\mathcal{K}}(q) = S^{\mathrm{T}}(q)\mathcal{K}(q), \tag{3.103}$$

and noting that $S^{\mathrm{T}}(q)B(q) = \mathbb{1}_2$, (3.100) is reduced to the form

$$\begin{aligned} \bar{\mathcal{M}}(q(t))\ddot{\eta}(t) + \bar{\mathcal{C}}(q(t),\dot{q}(t))\dot{\eta}(t) + \bar{\mathcal{K}}(q(t)) = \tau(t), \qquad q(0) = q_0, \qquad \dot{q}(0) = \dot{q}_0, \\ \eta(0) = [\mathbb{O}_{2\times 6}\mathbb{1}_2]q_0, \qquad \dot{\eta}(0) = [\mathbb{O}_{2\times 6}\mathbb{1}_2]\dot{q}_0. \end{aligned} \tag{3.104}$$

3.3 Conclusion

In this chapter, we discussed the studied the kinematics of the DDMR for planar motion in Section 3.1, and for non-planar motion in Section 3.2. Subsequently, the equations of motion were derived subject to the pure rolling and no slipping constraints.

Chapter 4

Adaptive control of a DDMR

In Chapter 3, we modeled the dynamics of the DDMR and derived its equations of motion. In this chapter, we design an adaptive controller for the DDMR to steer these system's dynamics. In Section 4.1, we discuss why we have chosen adaptive control as the control technique, Section 4.2 comprises of the reference model design, and finally a model reference adaptive control is designed in Section 4.3.

4.1 Motivation for an adaptive control law

The design of a controller for any dynamic system is based on some performance requirements for that system. The mathematical model of the dynamical system helps us understand and express the mechanism of the system approximately, and the degree to which the dynamical model approximates the actual system would dictate performance of the controller.

Any dynamical model is unavoidably approximate as there are uncertainties due to incomplete knowledge of some system parameters or unpredictable changes to the system or the surrounding. For instance, although the mass of the DDMR can be measured, it is usually difficult to detect the position of its center of mass as its components may have an unknown, non-uniform density and their exact location in the vehicle may be unknown. Furthermore, mobile robots may carry loads with unknown inertial parameters. We also can not predict

the effect of sling payloads on the overall system's dynamics. Aircraft or trucks experience considerable mass changes as they load or unload payloads or as the fuel is consumed. In order to control such systems, the controller should account for such parametric as well as modeling uncertainties. Adaptive control is one of the approaches that can account for the said uncertainties in the plant model. An adaptive control system basically estimates the unknown parameters on an on-line basis and computes the control inputs by employing the estimated parameters.

In this thesis, we aim to design a controller so that a DDMR follows the trajectory of an ideal reference model despite parametric and modeling uncertainties. Such control system is called model reference adaptive control (MRAC) system. A typical MRAC system is represented by Figure 4.1. It consists of a plant, a reference model, a feedback controller,

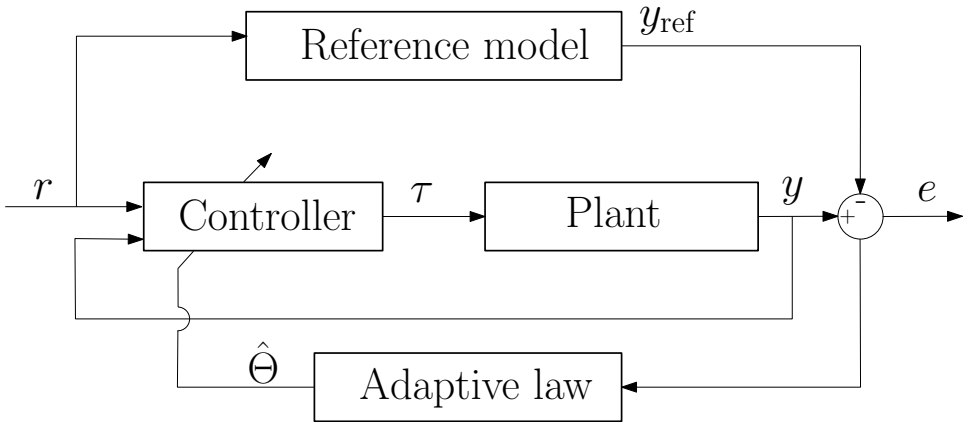

Figure 4.1: General structure of the MRAC architecture

and an adaptive law. We assume that at least the structure of the plant is known and its parameters are unknown. The reference model specifies the desired response of the control system. The controller is designed with the aim to reduce the tracking error, $e(t) \triangleq y(t) - y_{\text{ref}}(t), t \geq 0$, where y and y_{ref} denote the outputs of the plant and the reference model, respectively. The adaptive law is the adjustment mechanism used to generate the controller parameters on-line. We use a similar scheme to design a controller for the DDMR.

4.2 Reference model design

The first step towards designing MRAC is to generate a reference model of the system. The reference model describes the ideal system's behaviour. The dynamics of the DDMR can be captured by

$$\begin{aligned} \mathcal{M}(q(t))\ddot{q}(t) + \mathcal{C}(q(t),\dot{q}(t))\dot{q}(t) + \mathcal{K}(q(t)) &= A^{\mathrm{T}}(q(t))\lambda + B(q(t))\tau(t), \\ \begin{bmatrix} q(0) \\ \dot{q}(0) \end{bmatrix} &= \begin{bmatrix} q_0 \\ \dot{q}_0 \end{bmatrix}, \qquad t \geq 0. \end{aligned} \tag{4.1}$$

where $\tau \in \mathbb{R}^2$ denotes the control input to be designed using the MRAC architecture. Since $q \in \mathbb{R}^5$ for the planar case, and $q \in \mathbb{R}^8$ for the three-dimensional case, then we design the reference model for the general case of $q \in \mathbb{R}^n$.

The purpose of the reference model is to generate a twice continuously differentiable reference trajectory, $q_{\mathrm{ref}} : [0,\infty) \to \mathbb{R}^n$, which tracks the twice continuously differentiable user-defined trajectory, $q_{\mathrm{d}} : [0,\infty) \to \mathbb{R}^n$. We take the structure of the reference model from (4.1) and assume that all the states of the system can be actuated. Thus, we can take the reference model as

$$\hat{\mathcal{M}}(q_{\mathrm{ref}}(t))\ddot{q}_{\mathrm{ref}}(t) + \hat{\mathcal{C}}(q_{\mathrm{ref}}(t),\dot{q}_{\mathrm{ref}}(t))\dot{q}_{\mathrm{ref}}(t) + \hat{\mathcal{K}}(q_{\mathrm{ref}}(t)) = \tau_{\mathrm{ref}}(t), \quad \begin{bmatrix} q_{\mathrm{ref}}(0) \\ \dot{q}_{\mathrm{ref}}(0) \end{bmatrix} = \begin{bmatrix} q_{\mathrm{r0}} \\ \dot{q}_{\mathrm{r0}} \end{bmatrix}, \quad t \geq 0, \tag{4.2}$$

where $\hat{\mathcal{M}}(\cdot)$, $\hat{\mathcal{C}}(\cdot)$, and $\hat{\mathcal{K}}(\cdot)$ denote the user-defined estimates of $\mathcal{M}(\cdot)$, $\mathcal{C}(\cdot)$, and $\mathcal{K}(\cdot)$, respectively, and $\tau_{\mathrm{ref}} \in \mathbb{R}^n$ denotes the control input for the reference system.

To design $\tau_{\mathrm{ref}}(\cdot)$, we implement the inverse dynamics approach, which is based on the

cancellation of nonlinearities in the system dynamics. Specifically, we set

$$\tau_{\text{ref}}(t) = \hat{\mathcal{M}}(q_{\text{ref}}(t))\left[\ddot{q}_{\text{d}}(t) - K_P\left(q_{\text{ref}}(t) - q_{\text{d}}(t)\right) - K_D\left(\dot{q}_{\text{ref}}(t) - \dot{q}_{\text{d}}(t)\right)\right] + \hat{\mathcal{C}}(q_{\text{ref}}(t), \dot{q}_{\text{ref}}(t))\dot{q}_{\text{ref}}(t) + \hat{\mathcal{K}}(q_{\text{ref}}(t)), \qquad t \geq 0, \quad (4.3)$$

where K_P and $K_D \in \mathbb{R}^{n\times n}$ are user-defined, diagonal, and positive-definite. It follows from (4.2) and (4.3) that

$$\ddot{q}_{\text{ref}}(t) - \ddot{q}_{\text{d}}(t) + K_P\left(q_{\text{ref}}(t) - q_{\text{d}}(t)\right) + K_D\left(\dot{q}_{\text{ref}}(t) - \dot{q}_{\text{d}}(t)\right) = 0,$$
$$\begin{bmatrix} q_{\text{ref}}(0) \\ \dot{q}_{\text{ref}}(0) \end{bmatrix} = \begin{bmatrix} q_{\text{r0}} \\ \dot{q}_{\text{r0}} \end{bmatrix}, \quad \begin{bmatrix} q_{\text{d}}(0) \\ \dot{q}_{\text{d}}(0) \end{bmatrix} = \begin{bmatrix} q_{\text{d0}} \\ \dot{q}_{\text{d0}} \end{bmatrix}, \qquad t \geq 0. \quad (4.4)$$

Let

$$e(t) \triangleq \begin{bmatrix} q_{\text{ref}}(t) - q_{\text{d}}(t) \\ \dot{q}_{\text{ref}}(t) - \dot{q}_{\text{d}}(t) \end{bmatrix}, \qquad t \geq 0. \quad (4.5)$$

denote the trajectory tracking error. It follows from (4.4) and (4.5) that the error dynamics of the reference system as

$$\dot{e}(t) = \begin{bmatrix} 0 & \mathbb{1}_n \\ -K_P & -K_D \end{bmatrix} e(t), \qquad e(0) = e_0, \qquad t \geq 0. \quad (4.6)$$

The matrix $\begin{bmatrix} 0 & \mathbb{1}_n \\ -K_P & -K_D \end{bmatrix}$ is Hurwitz and thus, the the error dynamics is stable and the error exponentially converges to zero. This implies that using the controller in (4.3), we can generate a reference trajectory $q_{\text{ref}}(\cdot)$ that tracks the user-defined trajectory $q_d(\cdot)$.

4.3 Model reference adaptive control for a DDMR

In the reference model, we have assumed that all the states of the DDMR can be actuated. However, in practice, we can only control the motion of its wheels. Indeed, we obtained the reduced equations in the form of (3.49) and (3.104), for the planar and non-planar cases, respectively. From the reference model (4.2), we deduce the twice continuously differentiable reference trajectory, $q_{\text{ref}} : [0, \infty) \to \mathbb{R}^n$, and we obtain the reference trajectory for the wheels as $\eta_{\text{ref}}(t) \triangleq [\mathbb{O}_{2\times n-2} \;\; \mathbb{1}_2]\, q_{\text{ref}}(t),\ t \geq 0$. The reduced equations of motion of the DDMR are given by

$$\bar{\mathcal{M}}(q(t))\ddot{\eta}(t) + \bar{\mathcal{C}}(q(t), \dot{q}(t))\dot{\eta}(t) + \bar{\mathcal{K}}(q(t)) = \tau(t), \qquad \begin{bmatrix} q(0) \\ \dot{q}(0) \end{bmatrix} = \begin{bmatrix} q_0 \\ \dot{q}_0 \end{bmatrix}, \qquad t \geq 0, \tag{4.7}$$

where $\eta(t) \triangleq \begin{bmatrix} \mathbb{O}_{2\times(n-2)} & \mathbb{1}_2 \end{bmatrix} q(t)$.

Using equation (4.7), we can design a control law to govern the dynamics of the wheels of the DDMR, so that the error, $e_\eta(t) \triangleq \eta(t) - \eta_{\text{ref}}(t),\ t \geq 0$, asymptotically converges to zero. Even if the wheels of DDMR follow the reference trajectory, the global position of the DDMR might be different than the reference position. However, we are interested in designing a controller that makes the DDMR reach the global reference trajectory. To this goal, in the case of planar motion, we define the trajectory tracking error [25] in the reference frame $\mathbb{J}(\cdot)$ as

$$e(t) \triangleq \begin{bmatrix} e_1(t) \\ e_2(t) \\ e_3(t) \end{bmatrix} = \mathbf{R}^{\mathrm{T}}(\psi) \begin{bmatrix} X_{\text{ref}}(t) - X_A(t) \\ Y_{\text{ref}}(t) - Y_A(t) \\ \psi_{\text{ref}}(t) - \psi(t) \end{bmatrix}, \qquad t \geq 0, \tag{4.8}$$

where $X_{\text{ref}}(t), Y_{\text{ref}}(t)$, and $\psi_{\text{ref}}(t)$ denote the the reference trajectories of A along the X and Y axes, and the reference yaw angle of the DDMR, respectively. We aim to design a controller

to reduce $e(\cdot)$ to zero. The derivatives of the error terms [26] are obtained from (3.23) and (3.25) as

$$\dot{e}_1(t) = e_2(t)\dot{\psi}(t) - \dot{x}_A(t) + \dot{x}_{\text{ref}}(t)\cos e_3(t), \qquad t \geq 0, \tag{4.9}$$

$$\dot{e}_2(t) = -e_1(t)\dot{\psi}(t) + \dot{x}_{\text{ref}}(t)\sin e_3(t), \tag{4.10}$$

$$\dot{e}_3(t) = \dot{\psi}_{\text{ref}}(t) - \dot{\psi}(t), \tag{4.11}$$

where $\dot{x}_{\text{ref}}(t) \triangleq \begin{bmatrix} \frac{r}{2} & \frac{r}{2} \end{bmatrix} \dot{\eta}_{\text{ref}}(t)$, and $\dot{\psi}_{\text{ref}}(t) \triangleq \begin{bmatrix} \frac{r}{2w}, & -\frac{r}{2w} \end{bmatrix} \dot{\eta}_{\text{ref}}(t)$. We assume that $\dot{x}_{\text{ref}}(\cdot)$ and $\dot{\psi}_{\text{ref}}(\cdot)$ are not zero at the same time, and are bounded.

In order to drive $e(\cdot)$ to zero, we consider $\nu(t) \triangleq [\dot{x}_A(t) \;\; \dot{\psi}(t)]^{\mathrm{T}}$, $t \geq 0$, as an input in the equations (4.9)–(4.11). Thus, the dynamical model with $\nu(\cdot)$ as state variable can be obtained using (4.7), (3.23), and (3.25) as

$$\mathcal{M}_\nu(q(t))\dot{\nu}(t) + \mathcal{C}_\nu(q(t), \dot{q}(t))\nu(t) + \mathcal{K}_\nu(q(t)) = u(t), \qquad \begin{bmatrix} q(0) \\ \dot{q}(0) \\ \nu(0) \end{bmatrix} = \begin{bmatrix} q_0 \\ \dot{q}_0 \\ \nu_0 \end{bmatrix}, \qquad t \geq 0, \tag{4.12}$$

where $\mathcal{M}_\nu(q)$ denotes the *generalized mass matrix*, $\mathcal{C}_\nu(q, \dot{q})$ denotes the *centripetal and Coriolis matrix*, and $\mathcal{K}_\nu(q)$ denotes the *generalized gravitational force*; the expressions for $\mathcal{M}_\nu(\cdot)$, $\mathcal{C}_\nu(\cdot, \cdot)$, and $\mathcal{K}_\nu(\cdot)$ are omitted for brevity. Furthermore, we define

$$u(t) \triangleq \begin{bmatrix} \frac{1}{w} & \frac{1}{w} \\ 1 & -1 \end{bmatrix} \tau(t), \qquad t \geq 0. \tag{4.13}$$

We now design the controller $u(\cdot)$ to drive the linear and angular velocity vector $\nu(\cdot)$ to a desired velocity control $\nu_{\text{d}}(\cdot) \in \mathbb{R}^2$, chosen such that $e(\cdot)$ converges to zero. In particular, we

choose [27]

$$\nu_{\mathrm{d}}(t) \triangleq \begin{bmatrix} \dot{x}_{\mathrm{ref}}(t)\cos e_3(t) + k_1 e_1(t) \\ \dot{\psi}_{\mathrm{ref}}(t) + k_2 \dot{x}_{\mathrm{ref}}(t) e_2(t) + k_3 \sin e_3(t) \end{bmatrix}, \qquad t \geq 0, \tag{4.14}$$

where k_1, k_2, and k_3 are positive constants. The control error is defined as

$$\rho(t) \triangleq \nu_{\mathrm{d}}(t) - \nu(t), \qquad t \geq 0. \tag{4.15}$$

Differentiating (4.15) and multiplying by $\mathcal{M}_\nu(q(t))$, we obtain

$$\mathcal{M}_\nu(q(t))\dot{\rho}(t) = \mathcal{M}_\nu(q(t))\dot{\nu}_{\mathrm{d}}(t) - \mathcal{M}_\nu(q(t))\dot{\nu}(t), \qquad \rho(0) = \rho_0, \qquad t \geq 0. \tag{4.16}$$

Thus, it follows from (4.16), (4.15), and (4.12) that

$$\mathcal{M}_\nu(q(t))\dot{\rho}(t) = \mathcal{M}_\nu(q(t))\dot{\nu}_{\mathrm{d}}(t) + \mathcal{C}_\nu(q(t),\dot{q}(t))\nu_{\mathrm{d}}(t) - C_\nu(q(t),\dot{q}(t))\rho(t) + \mathcal{K}_\nu(q(t)) - u(t), \tag{4.17}$$

and we choose the controller as

$$u(t) = \begin{bmatrix} e_1(t) \\ \frac{1}{k_2}\sin e_3(t) \end{bmatrix} + \hat{\mathcal{M}}_\nu(q(t))\dot{\nu}_{\mathrm{d}}(t) + \hat{\mathcal{C}}_\nu(q(t),\dot{q}(t))\nu_{\mathrm{d}}(t) + \hat{\mathcal{K}}_\nu(q(t)) + K_0\rho(t) + \delta a(t), \qquad t \geq 0, \tag{4.18}$$

where $\hat{\mathcal{M}}_\nu(\cdot)$, $\hat{\mathcal{C}}_\nu(\cdot,\cdot)$, and $\hat{\mathcal{K}}_\nu(\cdot)$ denote the estimates of $\mathcal{M}_\nu(\cdot)$, $\mathcal{C}_\nu(\cdot,\cdot)$, and $\mathcal{K}_\nu(\cdot)$, respectively, $K_0 \in \mathbb{R}^{2\times 2}$ is a user-defined, positive definite, and diagonal, and $\delta a : [0,\infty) \to \mathbb{R}^2$ is an adaptive term to be defined. We know that mechanical systems are linear in their parameters [see 13, Sec 7.5.3] and hence, there exists $\mathcal{Y} : \mathbb{R}^2 \times \mathbb{R}^2 \times \mathbb{R}^n \times \mathbb{R}^n \to \mathbb{R}^{2\times N}$ and

$\widetilde{\Theta} \in \mathbb{R}^N$ such that

$$\widetilde{\mathcal{M}}_\nu(q)\dot{\nu}_{\mathrm{d}}+\widetilde{\mathcal{C}}_\nu(q,\dot{q})\nu_{\mathrm{d}}+\widetilde{\mathcal{K}}_\nu(q) = \mathcal{Y}(\nu_{\mathrm{d}},\dot{\nu}_{\mathrm{d}},q,\dot{q})\widetilde{\Theta}, \qquad (\nu_{\mathrm{d}},\dot{\nu}_{\mathrm{d}},q,\dot{q}) \in \mathbb{R}^2\times\mathbb{R}^2\times\mathbb{R}^n\times\mathbb{R}^n, \tag{4.19}$$

where

$$\widetilde{\mathcal{M}}_\nu(q) \triangleq \mathcal{M}_\nu(q) - \hat{\mathcal{M}}_\nu(q), \qquad (q,\dot{q}) \in \mathbb{R}^n \times \mathbb{R}^n, \tag{4.20}$$

$$\widetilde{\mathcal{C}}_\nu(q,\dot{q}) \triangleq \mathcal{C}_\nu(q,\dot{q}) - \hat{\mathcal{C}}_\nu(q,\dot{q}), \tag{4.21}$$

$$\widetilde{\mathcal{K}}_\nu(q) \triangleq \mathcal{K}_\nu(q) - \hat{\mathcal{K}}_\nu(q). \tag{4.22}$$

Now, the adaptive term is chosen as

$$\delta a(t) = \mathcal{Y}(\nu_{\mathrm{d}}(t),\dot{\nu}_{\mathrm{d}}(t),q(t),\dot{q}(t))\hat{\Theta}(t), \qquad t \geq 0, \tag{4.23}$$

where $\hat{\Theta} : [0,\infty) \to \mathbb{R}^N$ can be considered as the estimate of $\widetilde{\Theta}$. It follows from (4.18), (4.19), and (4.23) that

$$\begin{aligned} u(t) = {} & \begin{bmatrix} e_1(t) \\ \frac{1}{k_2}\sin e_3(t) \end{bmatrix} + \mathcal{M}_\nu(q(t))\dot{\nu}_{\mathrm{d}}(t) + \mathcal{C}_\nu(q(t),\dot{q}(t))\nu_{\mathrm{d}}(t) + \mathcal{K}_\nu(q(t)) + K_0\rho(t) \\ & - \mathcal{Y}(\nu_{\mathrm{d}}(t),\dot{\nu}_{\mathrm{d}}(t),q(t),\dot{q}(t))\Delta\Theta(t), \qquad \begin{bmatrix} q(0) \\ \dot{q}(0) \\ \nu_{\mathrm{d}}(0) \end{bmatrix} = \begin{bmatrix} q_0 \\ \dot{q}_0 \\ \nu_{\mathrm{d}0} \end{bmatrix}, \qquad t \geq 0, \end{aligned} \tag{4.24}$$

where $\Delta\Theta(t) \triangleq \widetilde{\Theta} - \hat{\Theta}(t)$.

To deduce an adaptive law for $\hat{\Theta}(\cdot)$, consider the Lyapunov function candidate

$$V(e,\rho,\hat{\Theta}) \triangleq \frac{1}{2}e_1^2 + \frac{1}{2}e_2^2 + \frac{1}{k_2}(1-\cos e_3) + \frac{1}{2}\rho^{\mathrm{T}}\mathcal{M}_\nu(q)\rho + \frac{1}{2}\Delta\Theta^{\mathrm{T}}\Gamma^{-1}\Delta\Theta, \\ (e,\rho,\hat{\Theta}) \in \mathbb{R}^3 \times \mathbb{R}^2 \times \mathbb{R}^N, \tag{4.25}$$

where $\Gamma \in \mathbb{R}^{N\times N}$ is symmetric and positive-definite. Differentiating (4.25) yields

$$\begin{aligned}\dot{V}(e(t),\rho(t),\hat{\Theta}(t)) &= e_1(t)(e_2(t)\dot{\psi}(t) - k_1e_1(t)) + e_2(t)(-e_1(t)\dot{\psi}(t) + \dot{x}_{\mathrm{ref}}(t)\sin e_3(t)) \\ &\quad + \frac{1}{k_2}\sin e_3(t)\left(-k_2\dot{x}_{\mathrm{ref}}(t)e_2(t) - k_3\sin e_3(t)\right) + \rho^{\mathrm{T}}(t)\begin{bmatrix} e_1(t) \\ \frac{1}{k_2}\sin e_3(t)\end{bmatrix} \\ &\quad + \rho^{\mathrm{T}}(t)\mathcal{M}_\nu(q(t))\dot{\rho}(t) + \frac{1}{2}\rho^{\mathrm{T}}\dot{\mathcal{M}}_\nu(q(t))\rho(t) - \Delta\Theta^{\mathrm{T}}\Gamma^{-1}\dot{\hat{\Theta}}(t), \\ &\quad t \geq 0. \end{aligned} \tag{4.26}$$

Thus, it follows from (4.26), (4.17), and (4.24) that

$$\begin{aligned}\dot{V}(e(t),\rho(t),\hat{\Theta}(t)) &= -k_1e_1^2(t) - \frac{k_3}{k_2}\sin^2 e_3(t) - \rho^{\mathrm{T}}(t)K_0\rho(t) \\ &\quad + \Delta\Theta^{\mathrm{T}}\left(\mathcal{Y}^{\mathrm{T}}(\nu_{\mathrm{d}}(t),\dot{\nu}_{\mathrm{d}}(t),q(t),\dot{q}(t))\rho(t) - \Gamma^{-1}\dot{\hat{\Theta}}(t)\right). \end{aligned} \tag{4.27}$$

We observe that if we select the adaptive law

$$\dot{\hat{\Theta}}(t) = \Gamma\mathcal{Y}^{\mathrm{T}}(\nu_{\mathrm{d}}(t),\dot{\nu}_{\mathrm{d}}(t),q(t),\dot{q}(t))\rho(t), \qquad \hat{\Theta}(0) = \hat{\Theta}_0, \qquad t \geq 0, \tag{4.28}$$

then it follows from (4.27) and (4.28) that

$$\begin{aligned}\dot{V}(e(t),\rho(t),\hat{\Theta}(t)) &= -k_1e_1^2(t) - \frac{k_3}{k_2}\sin^2 e_3(t) - \rho^{\mathrm{T}}(t)K_0\rho(t) \\ &\leq 0, \qquad t \geq 0, \end{aligned} \tag{4.29}$$

along all trajectories of (4.8), (4.15), and (4.28). Therefore, $e(t), t \geq 0, \rho(t)$, and $\hat{\Theta}(t)$ are bounded. The second derivative of the Lyapunov function (4.25) is obtained as

$$\begin{aligned}\ddot{V}(e(t),\rho(t),\hat{\Theta}(t)) = &-2k_1e_1(t)e_2(t)(\dot{\psi}_{\text{ref}}(t) + k_2\dot{x}_{\text{ref}}(t)e_2(t) + k_3\sin e_3(t) - [0 \;\; 1]\rho(t)) \\ &- 2k_1e_1(t)([1 \;\; 0]\rho(t) - k_1e_1(t)) - \frac{2k_3}{k_2}\sin e_3(t)\cos e_3(t)[0 \;\; 1]\rho(t) \\ &+ \frac{2k_3}{k_2}\sin e_3(t)\cos e_3(t)(k_2\dot{x}_{\text{ref}}(t)e_2(t) + k_3\sin e_3(t)) \\ &- 2\rho^{\mathrm{T}}(t)K_0\dot{\rho}(t), \qquad t \geq 0.\end{aligned} \tag{4.30}$$

Since $\dot{x}_{\text{ref}}(t)$, $\dot{\psi}_{\text{ref}}(t)$, $e(t)$, and $\rho(t)$ are bounded, $\ddot{V}(e(t),\rho(t),\hat{\Theta}(t))$ is bounded. Hence, $\dot{V}(e(t),\rho(t),\hat{\Theta}(t))$ is uniformly continuous and thus, it follows from Barbalat's lemma [see 28, Lemma 8.2] that $\lim_{t\to\infty}\rho(t) = 0$ and $\lim_{t\to\infty} e(t) = 0$.

In conclusion, we have proven that with $u(\cdot)$ given by (4.18), $\delta a(\cdot)$ given by (4.23), and adaptive gain $\hat{\Theta}(\cdot)$, the linear and angular velocities of the DDMR follow the desired controls $\nu_{\text{d}}(\cdot)$ which in turn drive the DDMR to the reference trajectory, so that (4.28) is verified. Ultimately, the torque inputs to the wheels of the DDMR are computed from equation (4.13).

4.4 Conclusion

In this chapter, we discussed the motivation behind the choice of model reference adaptive control. In Section 4.2, we designed the reference model describing ideal behaviour for the DDMR. In Section 4.3, we designed the adaptive controller that directs the DDMR to follow the reference trajectory.

Chapter 5

Dynamics of five-link robotic arms

The purpose of this chapter is to study the dynamics of a five-link robot arm and derive its equations of motion. First, we discuss the forward and and inverse kinematics of the robotic arm in Section 5.1, including the Denavit-Hartenberg convention, and then we derive the Euler-Lagrange equations of motion in Section 5.2.

5.1 Forward and inverse kinematics

Kinematics describe the motion of the manipulator employing just its geometry. In this thesis, a five-link robotic arm was used. The first link from the ground is called the *base link* and the frame attached to the base link is denoted by $\{\mathbf{o}_0; x_0(t), y_0(t), z_0\},\ t \geq 0$. The subsequent links are called the *shoulder*, the *forearm*, the *wrist*, and the *gripper*, respectively. Each of the links has a revolute joint and the frame of reference for the j^{th} link is denoted by $\{\mathbf{o}_j(t); x_j(t), y_j(t), z_j(t)\},\ t \geq 0,\ j = 1, \ldots, 4$. The last link of the robotic arm, that is, the gripper is the end-effector. It can be seen that the motions of wrist and gripper do not affect the position but only the orientation of the end-effector.

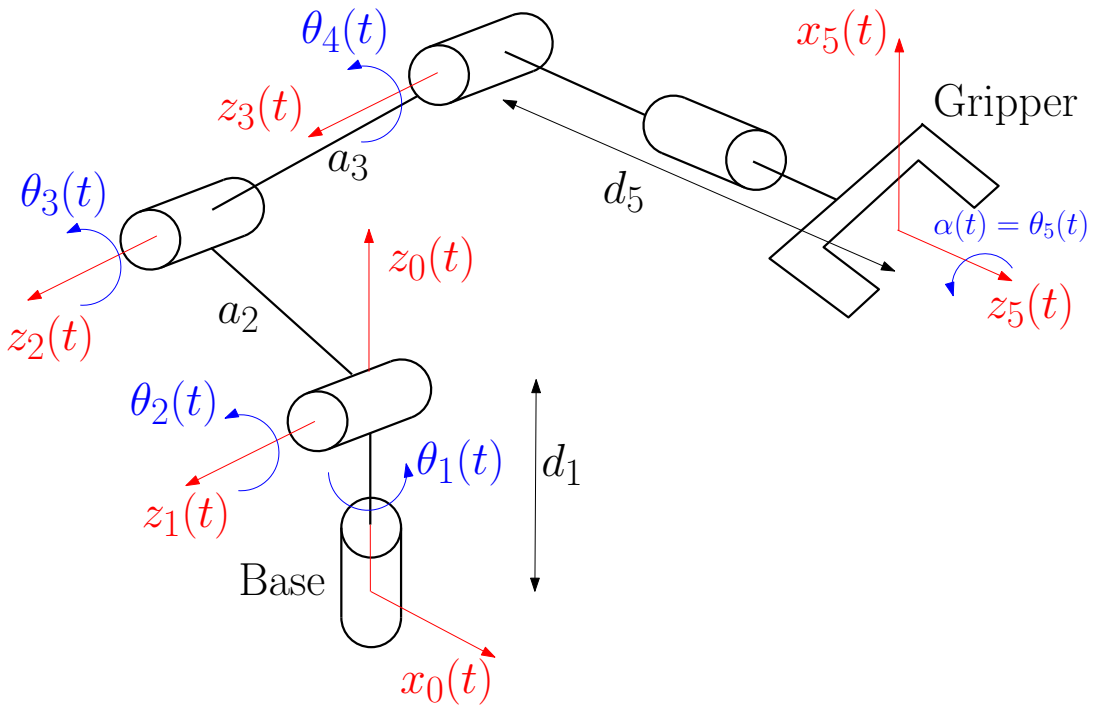

Figure 5.1: Schematic and frames assignment of the robotic arm.

5.1.1 The Denavit-Hartenberg convention and the forward kinematics

A commonly used convention for selecting frames of reference in robotic applications is the Denavit-Hartenberg, or DH convention; for additional details, see [13], Chapter 3. For a five-link robotic arm, the schematic and the allocation of the reference frame for each joint of the robotic arm considered in this thesis is illustrated in Figure 5.1. For each link i and joint i, there are four parameters associated with it, a_i, α_i, d_i, and θ_i, which are generally given the names *link length*, *link twist*, *link offset*, and *joint angle*, respectively. The Denavit-Hartenberg parameters for the robotic arm in Figure 5.1 are given in Table 5.1.

The forward kinematics problem concerns identifying the position and orientation of the end effector given the DH parameters characterizing the robot. For the robot considered on Figure 5.1, the joint variables are the angles between the links, $\theta_i(t), \quad i = 1, \ldots, 5, \quad t \geq 0$.

Table 5.1: DH parameters

Link	a_i	α_i	d_i	θ_i
1	0	$\pi/2$	d_1	$\theta_1(t)$
2	a_2	0	0	$\theta_2(t)$
3	a_3	0	0	$\theta_3(t)$
4	0	$\pi/2$	d_4	$\theta_4(t)$
5	0	0	d_5	$\theta_5(t)$

The corresponding homogeneous transformation between the center of the end-effector and the base is given by

$$T_5^0(t) = T_1^0(t)T_2^1(t)T_3^2(t)T_4^3(t)T_5^4(t), \qquad t \geq 0, \tag{5.1}$$

where

$$T_i^{i-1}(t) \triangleq \mathrm{Rot}_z(\theta_i(t))\mathrm{Tran}_z(d_i(t))\mathrm{Tran}_x(a_i(t))\mathrm{Rot}_x(\alpha_i(t)), \qquad i = 1, \ldots, 5, \tag{5.2}$$

$$\mathrm{Rot}_z(\theta_i(t)) \triangleq \begin{bmatrix} \begin{bmatrix} \cos\theta_i(t) & -\sin\theta_i(t) & 0 \\ \sin\theta_i(t) & \cos\theta_i(t) & 0 \\ 0 & 0 & 1 \end{bmatrix} & \begin{bmatrix} 0 \\ 0 \\ 0 \end{bmatrix} \\ [0 \quad 0 \quad 0] & 1 \end{bmatrix}, \tag{5.3}$$

$$\mathrm{Tran}_z(d_i(t)) \triangleq \begin{bmatrix} \begin{bmatrix} 1 & 0 & 0 \\ 0 & 1 & 0 \\ 0 & 0 & 1 \end{bmatrix} & \begin{bmatrix} 0 \\ 0 \\ d_i(t) \end{bmatrix} \\ [0 \quad 0 \quad 0] & 1 \end{bmatrix}, \tag{5.4}$$

$$\mathrm{Tran}_x(a_i(t)) \triangleq \begin{bmatrix} \begin{bmatrix} 1 & 0 & 0 \\ 0 & 1 & 0 \\ 0 & 0 & 1 \end{bmatrix} & \begin{bmatrix} a_i(t) \\ 0 \\ 0 \end{bmatrix} \\ [0 \quad 0 \quad 0] & 1 \end{bmatrix}, \tag{5.5}$$

$$\mathrm{Rot}_x(\theta_i(t)) \triangleq \begin{bmatrix} \begin{bmatrix} 1 & 0 & 0 \\ 0 & \cos\alpha_i(t) & -\sin\alpha_i(t) \\ 0 & \sin\alpha_i(t) & \cos\alpha_i(t) \end{bmatrix} & \begin{bmatrix} 0 \\ 0 \\ 0 \end{bmatrix} \\ [0 \quad 0 \quad 0] & 1 \end{bmatrix}. \tag{5.6}$$

Using (5.3)–(5.6), the homogeneous transformation in (5.2) can be written as

$$T_i^{i-1} = \begin{bmatrix} \mathbf{R}_i^{i-1} & \mathbf{o}_i^{i-1} \\ \mathbb{O}_{1\times 3} & 1 \end{bmatrix}, \tag{5.7}$$

where $\mathbf{R}_i^{i-1} \in \mathbb{R}^{3\times 3}$ denotes the rotation matrix between the i^{th} and $(i-1)^{th}$ frames, and $\mathbf{o}_i^{i-1} \in \mathbb{R}^3$ denotes the coordinates of the origin of the $(i-1)^{th}$ frame with respect to the i^{th} frame. Employing the DH convention, it holds that

$$\mathbf{R}_i^{i-1} \triangleq \begin{bmatrix} \cos\theta_i & -\sin\theta_i\cos\alpha_i & \sin\theta_i\sin\alpha_i \\ \sin\theta_i & \cos\theta_i\cos\alpha_i & \cos\theta_i\sin\alpha_i \\ 0 & \sin\alpha_i & \cos\alpha_i \end{bmatrix}, \tag{5.8}$$

$$\mathbf{o}_i^{i-1} \triangleq \begin{bmatrix} a_i\cos\theta_i \\ a_i\sin\theta_i \\ d_i \end{bmatrix}. \tag{5.9}$$

Thus, (5.1) can be computed as

$$T_5^0(t) = \begin{bmatrix} \mathbf{R}_5^0(t) & \mathbf{o}_5^0(t) \\ \mathbb{O}_{1\times 3} & 1 \end{bmatrix}, \qquad t \geq 0, \tag{5.10}$$

where the columns of $\mathbf{R}_5^0(t), \quad t \geq 0$, represent the coordinate axes of the frame attached to the end-effector, expressed in the base reference frame. Thus, we can solve the forward

kinematics of the robotic arm using (5.10), given the joint variables of the robotic arm.

5.1.2 Inverse kinematics

In Section 5.1.1, we showed how to determine the end effector's position and orientation in terms of the joint variables. In this subsection, we solve the inverse kinematics problem for the robotic arm, that is, we find the joint variables that realize the desired end effector's position and orientation.

In this case, we solve the inverse kinematics problem given $p^0(t) \in \mathbb{R}^3, \quad t \geq 0$, the desired position of the end effector, $z_5^0(t) \in \mathbb{R}^3$, the direction of the third axis of the gripper, and $\alpha(t) \in [0, 2\pi)$, the desired rotation angle of the gripper, all expressed in the reference frame $\{\mathbf{o}_0; x_0(t), y_0(t), z_0\}$. Let $p^0(t) = [p_x(t) \quad p_y(t) \quad p_z(t) + d_1]^{\mathrm{T}}$ and $z_5^0(t) = [z_{5,x}(t) \;\; z_{5,y}(t) \;\; z_{5,z}(t)]^{\mathrm{T}}$.

We observe that both $z_5(\cdot)$ and z_0 are coplanar. Thus, it holds that

$$\theta_1(t) = \tan^{-1}\left(\frac{p_y(t)}{p_x(t)}\right), \qquad t \geq 0, \tag{5.11}$$

and

$$\theta_5(t) = \alpha(t). \tag{5.12}$$

where $\tan^{-1}(\frac{\cdot}{\cdot})$ denotes the signed inverse tangent function. Thus, let

$$z_{5,X}(t) \triangleq \sqrt{z_{5,x}^2(t) + z_{5,y}^2(t)}, \qquad t \geq 0, \tag{5.13}$$

$$p_X(t) \triangleq \sqrt{p_x^2(t) + p_y^2(t)}. \tag{5.14}$$

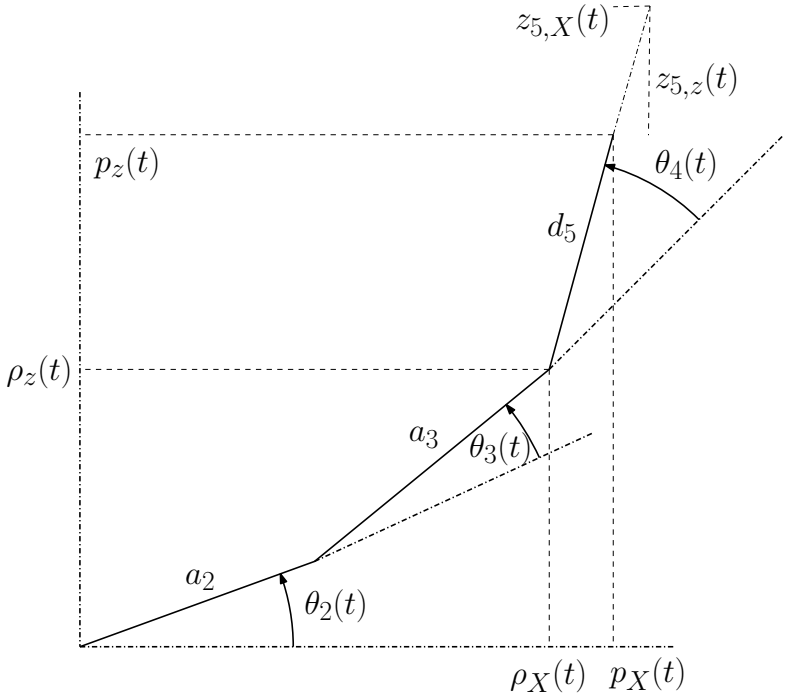

Figure 5.2: Schematic representation of the arm's side view.

We note that

$$p_X(t) = a_2 \cos\theta_2(t) + a_3 \cos\left(\theta_2(t) + \theta_3(t)\right) + d_5 \cos\beta(t), \qquad t \geq 0, \tag{5.15}$$

$$p_z(t) = a_2 \sin\theta_2(t) + a_3 \sin\left(\theta_2(t) + \theta_3(t)\right) + d_5 \sin\beta(t), \tag{5.16}$$

$$\beta(t) \triangleq \theta_2(t) + \theta_3(t) + \theta_4(t) = \tan^{-1}\left(\frac{z_{5,z}(t)}{z_{5,X}(t)}\right), \tag{5.17}$$

and hence,

$$\rho_X(t) \triangleq p_X(t) - d_5 \cos\beta(t) = a_2 \cos\theta_2(t) + a_3 \cos\left(\theta_2(t) + \theta_3(t)\right), \tag{5.18}$$

$$\rho_z(t) \triangleq p_z(t) - d_5 \sin\beta(t) = a_2 \sin\theta_2(t) + a_3 \sin\left(\theta_2(t) + \theta_3(t)\right), \tag{5.19}$$

where $p_X(\cdot)$, $p_z(\cdot)$, $\rho_X(\cdot)$, and $\rho_z(\cdot)$ are shown in Figure 5.2. Therefore, it follows from (5.18)

and (5.19) that

$$a_3^2 = [\rho_X(t) - a_2 \cos\theta_2(t)]^2 + [\rho_z(t) - a_2 \sin\theta_2(t)]^2, \qquad t \geq 0, \tag{5.20}$$

and

$$\theta_2(t) + \theta_3(t) = \tan^{-1}\left(\frac{\rho_z(t) - a_2 \sin\theta_2(t)}{\rho_X(t) - a_2 \cos\theta_2(t)}\right). \tag{5.21}$$

Consequently, expanding the right-hand side of (5.20), we obtain that

$$\rho_X(t)\cos\theta_2(t) + \rho_z(t)\sin\theta_2(t) = \frac{\rho_X^2(t) + \rho_z^2(t) + a_2^2 - a_3^2}{2a_2}, \qquad t \geq 0. \tag{5.22}$$

Now, let $\gamma(t) \triangleq \tan\frac{\theta_2(t)}{2}$ and

$$C(t) \triangleq \frac{\rho_X^2(t) + \rho_z^2(t) + a_2^2 - a_3^2}{2a_2}, \qquad t \geq 0. \tag{5.23}$$

In this case, it holds that

$$\sin\theta_2(t) = \frac{2\gamma(t)}{1+\gamma^2(t)}, \qquad t \geq 0, \tag{5.24}$$

$$\cos\theta_2(t) = \frac{1-\gamma^2(t)}{1+\gamma^2(t)}, \tag{5.25}$$

and hence, it follows from (5.22) that

$$[\rho_X(t) + C(t)]^2\gamma^2(t) - 2\rho_z(t)\gamma(t) + C(t) - \rho_X(t) = 0, \tag{5.26}$$

which implies that

$$\theta_2(t) = 2\tan^{-1}\left(\frac{\rho_z(t) \pm \sqrt{\rho_z^2(t) + \rho_X^2(t) - C^2(t)}}{\rho_X(t) + C(t)}\right). \tag{5.27}$$

Now, it follows from (5.21) and (5.27) that

$$\theta_3(t) = \tan^{-1}\left(\frac{\rho_z(t) - a_2\sin\theta_2(t)}{\rho_X(t) - a_2\cos\theta_2(t)}\right) - 2\tan^{-1}\left(\frac{\rho_z(t) \pm \sqrt{\rho_z^2(t) + \rho_X^2(t) - C^2(t)}}{\rho_X(t) + C(t)}\right), \quad t \geq 0. \tag{5.28}$$

Lastly, we can compute $\theta_4(t)$ from (5.17), (5.27), and (5.28) as

$$\theta_4(t) = \beta(t) - \theta_2(t) - \theta_3(t), \qquad t \geq 0. \tag{5.29}$$

Thus, in conclusion, given $p^0(t) = [p_x(t) \quad p_y(t) \quad p_z(t) + d_1]^{\mathrm{T}}$, $t \geq 0$, the unit vector $z_5^0(t) = [z_{5,x}(t) \quad z_{5,y}(t) \quad z_{5,z}(t)]^{\mathrm{T}}$, and $\alpha(t)$, we have computed the parameters that realize this configuration in (5.11), (5.27), (5.28), (5.29), and (5.12).

5.2 Equations of motion

The vector of generalized coordinates for the robotic arm is defined as

$$q \triangleq [\theta_1 \quad \theta_2 \quad \theta_3 \quad \theta_4 \quad \theta_5]^{\mathrm{T}}. \tag{5.30}$$

The linear and angular velocities of the center of mass of the i^{th} link can be respectively defined as

$$v_i(t) \triangleq J_{v_i}(q(t))\dot{q}(t), \qquad t \geq 0, \tag{5.31}$$

$$\omega_i(t) \triangleq J_{\omega_i}(q(t))\dot{q}(t), \tag{5.32}$$

where $J_{v_i}(q), J_{\omega_i}(q) \in \mathbb{R}^{3\times 5}$ are the linear and angular manipulator Jacobian matrices, respectively.

The robotic arm consists of five links, all of which have revolute joints. In this case, it follows that, for the i^{th} link, the j^{th} column of the linear Jacobian matrix, $J_{v_i}(q)$, is given by

$$J_{v_i,j} = \begin{cases} \left(z_{j-1}^0\right)^{\times} \left(\mathbf{o}_{c_i}^0 - \mathbf{o}_{j-1}^0\right) & ,\forall\, i \geq j, \\ \mathbb{O}_{3\times 1} & ,\forall\, j > i, \end{cases} \tag{5.33}$$

where $z_{j-1}^0 \in \mathbb{R}^3$ denotes the third axis of the $(j-1)^{th}$ reference frame expressed with respect to the base frame, $\mathbf{o}_{c_i}^0 \in \mathbb{R}^3$ denotes the coordinates of the center of mass of the i^{th} link expressed with respect to the base frame, and $\mathbf{o}_{j-1}^0 \in \mathbb{R}^3$ denotes the coordinates of the origin of the $(j-1)^{th}$ frame with respect to the base frame Spong et al. [13, chap. 4]. For the i^{th} link, the j^{th} column of the angular Jacobian matrix, $J_{\omega_i}(q)$, is given by

$$J_{\omega_i,j} = \begin{cases} z_{j-1}^0 & ,\forall\, i \geq j, \\ \mathbb{O}_{3\times 1} & ,\forall\, j > i, \end{cases} \tag{5.34}$$

Using (5.33) and (5.34), we get five linear Jacobian matrices and five angular Jacobian matrices. The overall kinetic energy, $T : \mathbb{R}^5 \times \mathbb{R}^5 \to \mathbb{R}$, of the robotic arm is given by

$$T(q,\dot{q}) = \frac{1}{2}\dot{q}^{\mathrm{T}} \left[\sum_{i=1}^{5} \left(m_i J_{v_i}^{\mathrm{T}}(q) J_{v_i}(q) + I_i J_{\omega_i}^{\mathrm{T}}(q) J_{\omega_i}(q)\right)\right] \dot{q}, \qquad (q,\dot{q}) \in \mathbb{R}^5 \times \mathbb{R}^5, \tag{5.35}$$

where $m_i > 0$ denotes the mass of the i^{th} link, and $I_i > 0$ denotes the moment of inertia about an axis through the center of mass of link i parallel to the z_i-axis. The overall potential

energy of the robotic arm, $U : \mathbb{R}^5 \to \mathbb{R}$, is given by

$$U(q) = \sum_{i=1}^{5} m_i (g z_0^0)^{\mathrm{T}} \mathbf{o}_{c_i}^0, \qquad q \in \mathbb{R}^5, \tag{5.36}$$

where $g > 0$ denotes the gravitational acceleration. The *Lagrangian* function for the robotic arm is given by

$$\mathcal{L}(q, \dot{q}) = T(q, \dot{q}) - U(q), \qquad (q, \dot{q}) \in \mathbb{R}^5 \times \mathbb{R}^5. \tag{5.37}$$

The Euler-Lagrange equations of motion for the robotic arm can be written as

$$\mathcal{M}(q)\ddot{q} + \mathcal{C}(q, \dot{q})\dot{q} + \mathcal{K}(q) = \tau, \qquad q(0) = q_0, \qquad \dot{q}(0) = \dot{q}_0, \tag{5.38}$$

where $\mathcal{M}(q)$ denotes the *generalized mass matrix*, $\mathcal{C}(q, \dot{q})$ denotes the *centripetal and Coriolis matrix* , $\mathcal{K}(q)$ denotes the *gravitational force* matrix, and $\tau \in \mathbb{R}^5$ denotes the input vector comprising of torques such that

$$\mathcal{M}(q) \triangleq \left[\sum_{i=1}^{5} \left(m_i J_{v_i}^{\mathrm{T}}(q) J_{v_i}(q) + I_i J_{\omega_i}^{\mathrm{T}}(q) J_{\omega_i}(q) \right) \right], \tag{5.39}$$

$$\mathcal{K}(q) \triangleq \frac{\partial U(q)}{\partial q}, \tag{5.40}$$

and the $(k, j)^{th}$ element of the matrix $\mathcal{C}(q, \dot{q})$ is defined as

$$c_{kj} \triangleq \frac{1}{2} \sum_{i=1}^{5} \left(\frac{\partial M_{kj}}{\partial q_i} + \frac{\partial M_{ki}}{\partial q_j} - \frac{\partial M_{ij}}{\partial q_k} \right) \dot{q}_i, \tag{5.41}$$

where M_{kj} denotes the $(k, j)^{th}$ element of $\mathcal{M}(q)$; the expressions for $\mathcal{M}(\cdot)$, $\mathcal{C}(\cdot, \cdot)$, and $\mathcal{K}(\cdot)$ for the five-link robot shown in Figure 5.1 are omitted for brevity.

5.3 Conclusion

In this chapter, the forward and inverse kinematics for the five-link robotic arm are derived with the help of DH parameters in Section 5.1. Then, in Section 5.2, we derived the equations of motion for the robotic arm.

Chapter 6

Adaptive control of five-link robotic arms

In this chapter, we design an adaptive controller for robotic arms, such as a five-link robotic arm. As discussed in Chapter 5, the equations of motion of the robotic arm are captured by

$$\mathcal{M}(q(t))\ddot{q}(t) + \mathcal{C}(q(t), \dot{q}(t))\dot{q}(t) + \mathcal{K}(q(t)) = \tau(t), \qquad \begin{bmatrix} q(0) \\ \dot{q}(0) \end{bmatrix} = \begin{bmatrix} q_0 \\ \dot{q}_0 \end{bmatrix}, \qquad t \geq 0, \tag{6.1}$$

In order to design a nonlinear feedback control law for this system, we use the inverse dynamics control approach. However, for this methodology to be implemented, we need to have complete knowledge of the system parameters, and, as discussed in Section 4.1, there are uncertainties in the parameters. Therefore, we use the estimates of the nominal parameter values to design an inverse dynamics control law and add an adaptive term to account for the resulting uncertainties. We choose the control input as

$$\tau(t) = \hat{\mathcal{M}}(q(t))a(t) + \hat{\mathcal{C}}(q(t), \dot{q}(t))v(t) + \hat{\mathcal{K}}(q(t)) - K_0\rho(t) + \delta a(t), \qquad t \geq 0, \tag{6.2}$$

where $\hat{\mathcal{M}}(\cdot)$, $\hat{\mathcal{C}}(\cdot)$, and $\hat{\mathcal{K}}(\cdot)$ denote the user-defined estimates of $\mathcal{M}(\cdot)$, $\mathcal{C}(\cdot)$, and $\mathcal{K}(\cdot)$, re-

spectively,

$$v(t) \triangleq \dot{q}_{\text{ref}}(t) - K_1 \tilde{q}(t), \tag{6.3}$$

$$a(t) \triangleq \ddot{q}_{\text{ref}}(t) - K_1 \dot{\tilde{q}}(t) = \dot{v}(t), \tag{6.4}$$

$$\rho(t) \triangleq \dot{q}(t) - v(t) = \dot{\tilde{q}} + K_1 \tilde{q}(t), \tag{6.5}$$

K_0 and $K_1 \in \mathbb{R}^{5\times 5}$ are user-defined, diagonal, and positive-definite, $\tilde{q}(t) \triangleq q(t) - q_{\text{ref}}(t)$, $q_{\text{ref}} : [0, \infty) \to \mathbb{R}^5$ denotes the twice continuously differentiable reference trajectory, and $\delta a : [0, \infty) \to \mathbb{R}^5$ denotes the adaptive term.

Using the definitions (6.3), (6.4), and (6.5), it follows from (6.1) and (6.2) that

$$\begin{aligned} &\mathcal{M}(q(t))\dot{\rho}(t) + \mathcal{C}(q(t), \dot{q}(t))\rho(t) + K_0\rho(t) \\ &\quad = \delta a(t) + \left[\widetilde{\mathcal{M}}(q(t))a(t) + \widetilde{\mathcal{C}}(q(t), \dot{q}(t))v(t) + \widetilde{\mathcal{K}}(q(t))\right], \qquad \rho(0) = \rho_0, \qquad t \geq 0, \end{aligned} \tag{6.6}$$

where

$$\widetilde{\mathcal{M}}(q) \triangleq \hat{\mathcal{M}}(q) - \mathcal{M}(q), \qquad (q, \dot{q}) \in \mathbb{R}^5 \times \mathbb{R}^5, \tag{6.7}$$

$$\widetilde{\mathcal{C}}(q, \dot{q}) \triangleq \hat{\mathcal{C}}(q, \dot{q}) - \mathcal{C}(q, \dot{q}), \tag{6.8}$$

$$\widetilde{\mathcal{K}}(q) \triangleq \hat{\mathcal{K}}(q) - \mathcal{K}(q). \tag{6.9}$$

Since mechanical systems are linear in their parameters, we can write

$$\widetilde{\mathcal{M}}(q)a + \widetilde{\mathcal{C}}(q, \dot{q})v + \widetilde{\mathcal{K}}(q) = \mathcal{Y}(v, a, q, \dot{q})\widetilde{\Theta}, \qquad (v, a, q, \dot{q}) \in \mathbb{R}^5 \times \mathbb{R}^5 \times \mathbb{R}^5 \times \mathbb{R}^5, \tag{6.10}$$

where $\mathcal{Y} : \mathbb{R}^5 \times \mathbb{R}^5 \times \mathbb{R}^5 \times \mathbb{R}^5 \to \mathbb{R}^{5\times 14}$ and $\widetilde{\Theta} \in \mathbb{R}^{14}$ for a five-link robotic arm, and thus,

$$\mathcal{M}(q(t))\dot{\rho}(t) + \mathcal{C}(q(t),\dot{q}(t))\rho(t) + K_0\rho(t)$$
$$= \delta a(t) + \mathcal{Y}(v(t),a(t),q(t),\dot{q}(t))\widetilde{\Theta}, \qquad \rho(0) = \rho_0, \qquad t \geq 0. \quad (6.11)$$

Now, the adaptive term is chosen as

$$\delta a(t) = -\mathcal{Y}(v(t),a(t),q(t),\dot{q}(t))\hat{\Theta}(t), \qquad t \geq 0, \quad (6.12)$$

where $\hat{\Theta} : [0,\infty) \to \mathbb{R}^{14}$ can be considered as the estimate of $\widetilde{\Theta}$.

It follows from (6.11) and (6.12) that

$$\bar{\mathcal{M}}(q(t))\dot{\rho}(t) + \bar{\mathcal{C}}(q(t),\dot{q}(t))\rho(t) + K_0\rho(t) = \mathcal{Y}(v(t),a(t),q(t),\dot{q}(t))\Delta\Theta(t),$$
$$\rho(0) = \rho_0, \qquad t \geq 0, \quad (6.13)$$

where $\Delta\Theta(t) \triangleq \widetilde{\Theta} - \hat{\Theta}(t)$.

In order to find $\hat{\Theta}(\cdot)$ such that $\rho(\cdot)$ is uniformly bounded for all initial conditions $\rho_0 \in \mathbb{R}^n$ and $\rho(t) \to 0$ as $t \to \infty$, consider the Lyapunov function candidate

$$V(\tilde{q},\rho,\hat{\Theta}) \triangleq \frac{1}{2}\rho^{\mathrm{T}}\mathcal{M}(q)\rho + \tilde{q}^{\mathrm{T}}K_1K_0\tilde{q} + \frac{1}{2}\Delta\Theta^{\mathrm{T}}\Gamma\Delta\Theta, \qquad (\tilde{q},\rho,\hat{\Theta}) \in \mathbb{R}^5 \times \mathbb{R}^5 \times \mathbb{R}^{14}, \quad (6.14)$$

where $\Gamma \in \mathbb{R}^{14\times 14}$ is symmetric and positive-definite. Differentiating (6.14) yields

$$\dot{V}(\tilde{q}(t),\rho(t),\hat{\Theta}(t)) = \rho^{\mathrm{T}}\bar{\mathcal{M}}(q(t))\dot{\rho}(t) + \frac{1}{2}\rho^{\mathrm{T}}\dot{\bar{\mathcal{M}}}(q(t))\rho(t) + 2\tilde{q}^{\mathrm{T}}K_1K_0\dot{\tilde{q}}(t) - \Delta\Theta^{T}\Gamma\dot{\hat{\Theta}}(t)$$
$$= \rho^{\mathrm{T}}[\mathcal{Y}(v(t),a(t),q(t),\dot{q}(t))\Delta\Theta(t) - \bar{\mathcal{C}}(q(t),\dot{q}(t))\rho(t) - K_0\rho(t)]$$
$$+ \frac{1}{2}\rho^{\mathrm{T}}\dot{\bar{\mathcal{M}}}(q(t))\rho(t) + 2\tilde{q}^{\mathrm{T}}K_1K_0\dot{\tilde{q}}(t) - \Delta\Theta^{\mathrm{T}}\Gamma\dot{\hat{\Theta}}(t)$$
$$= -\dot{\tilde{q}}^{\mathrm{T}}K_0\dot{\tilde{q}}(t) - \tilde{q}^{\mathrm{T}}K_1K_0K_1\tilde{q}(t)$$

$$+ \Delta\Theta^{\mathrm{T}} \left[\mathcal{Y}^{\mathrm{T}}(v(t), a(t), q(t), \dot{q}(t))\rho(t) - \Gamma\dot{\hat{\Theta}}(t) \right], \qquad t \geq 0. \tag{6.15}$$

We observe that if we select the adaptive law

$$\dot{\hat{\Theta}}(t) = \Gamma^{-1}\mathcal{Y}^{\mathrm{T}}(v(t), a(t), q(t), \dot{q}(t))\rho(t), \qquad \hat{\Theta}(0) = \hat{\Theta}_0, \qquad t \geq 0, \tag{6.16}$$

then it follows from (6.15) and (6.16) that

$$\begin{aligned} \dot{V}(\tilde{q}(t), \rho(t), \hat{\Theta}(t)) &= -\dot{\tilde{q}}^{\mathrm{T}} K_0 \dot{\tilde{q}}(t) - \tilde{q}^{\mathrm{T}} K_1 K_0 K_1 \tilde{q}(t) \\ &\leq 0, \qquad t \geq 0, \end{aligned} \tag{6.17}$$

along all trajectories of (6.13), (6.16), and (6.5). Therefore, $\tilde{q}(t), t \geq 0, \rho(t)$, and $\hat{\Theta}(t)$ are bounded. Therefore, it follows from (6.3) and (6.4) that $v(t), t \geq 0$, and $a(t)$ are bounded. Furthermore, we note that $\mathcal{Y}(\cdot, \cdot, \cdot, \cdot)$ is continuously differentiable and hence, it follows from (6.13) that $\dot{\rho}(t), t \geq 0$, is bounded and hence, $\dot{V}(\tilde{q}(t), \rho(t), \hat{\Theta}(t)) = -\dot{\tilde{q}}^{\mathrm{T}} K_0 \dot{\tilde{q}}(t) - \tilde{q}^{\mathrm{T}} K_1 K_0 K_1 \tilde{q}(t)$ is bounded, which implies that $\dot{V}(\cdot)$ is uniformly continuous. Lastly, it follows from Barbalat's lemma [see 28, Lemma 8.2] that $\lim_{t\to\infty} \rho(t) = 0$ and $\lim_{t\to\infty} \|q(t) - q_{\mathrm{ref}}(t)\| = 0$, and it follows from (6.5) that $\lim_{t\to\infty} \|\dot{q}(t) - \dot{q}_{\mathrm{ref}}(t)\| = 0$.

In conclusion, we have proven that the trajectory $q(\cdot)$ of mechanical system (6.1) can be steered to follow the reference trajectory $q_{\mathrm{ref}}(\cdot)$ with $\tau(\cdot)$ given by (6.2), $\delta a(\cdot)$ given by (6.12), and adaptive gain $\hat{\Theta}(\cdot)$, so that (6.16) is verified.

Chapter 7

Simulation and experimental results

In this thesis, we validate the control laws presented in Chapters 4 and 6 by considering a mobile manipulator comprising a DDMR and a five-degrees-of-freedom robotic arm. The dynamics of the DDMR and the robotic arm are considered to be decoupled and hence, their controllers are designed individually. We begin with computation of the desired trajectories for the DDMR and the robotic arm respectively in Section 7.1, followed by plots of the simulation results in Section 7.2, and experimental results in Section 7.3.

7.1 Reference trajectory generation

In order to perform numerical simulations and experiments, we need to derive twice continuously differentiable reference trajectories for the DDMR in the reference frame $\mathbb{I}$. We model the desired trajectory such that the DDMR moves in a straight line with a constant speed $v_{\text{ref}}(t) > 0,\ t \geq 0$, and we also model the desired trajectory so that the DDMR moves along a square with turns of radius $R_d > 0$, as illustrated in Figure 7.1. This twice continuously differentiable desired trajectory of the DDMR is then used to derive the reference system as discussed in Section 4.2.

For the robotic arm, we choose the reference trajectory directly. We want the trajectory for the robotic arm to be twice continuously differentiable and it should pass through a sequence of configurations or waypoints, which are chosen as follows. The robotic arm starts

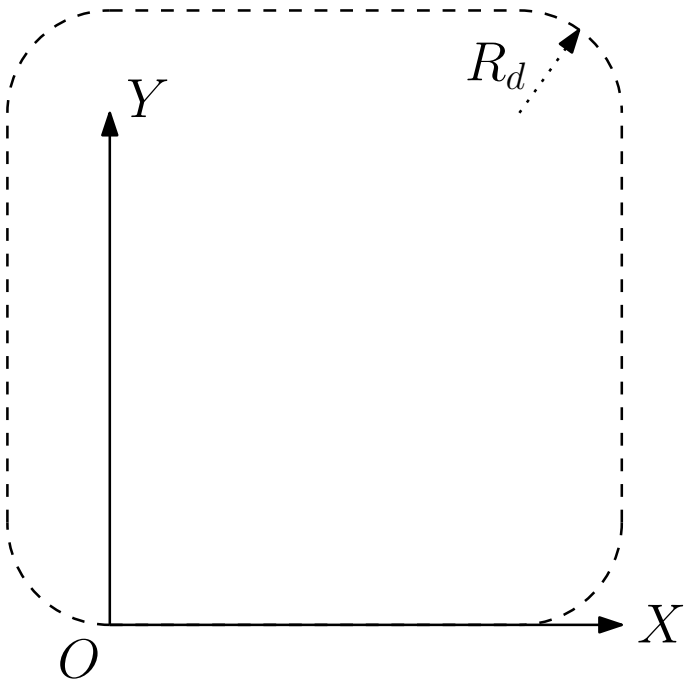

Figure 7.1: Schematic diagram of DDMR desired trajectory

with some initial configuration at $t = t_0$, then it moves so as to align the $z_5^0 \in \mathbb{R}^3$ axis with the $x_0^0 \in \mathbb{R}^3$ axis at $t = t_1$. After this, the robotic arm rotates along its $z_0^0 \in \mathbb{R}^3$ axis with a constant angular velocity to traverse an angle of $\frac{5\pi}{9}$ at $t = t_2$, followed by rising up and traversing angle of $\frac{4\pi}{9}$ with same angular speed at $t = t_3$. Thus, the reference trajectory has 4 waypoints at t_0, t_1, t_2, t_3, respectively. At each waypoint, we specify the position of the end-effector $p_i^0 \in \mathbb{R}^3$, that is, third axis of the gripper $z_{5,i}^0 \in \mathbb{R}^3$, and its orientation $\theta_{5,i} \in [0, 2\pi)$, and then using the inverse kinematics from Section 5.1.2, we obtain the desired joint variables $q_{d,i}$ at the waypoints. We also specify the angular velocities $\dot{q}_{d,i}$. The segment of the reference trajectory between the times $t = t_i$ and $t = t_{i-1}$, $i = 1, \ldots, 3$, for the constraints

$$q_{\text{ref}}(t_{i-1}) = q_{d,i-1}, \tag{7.1}$$

$$\dot{q}_{\text{ref}}(t_{i-1}) = \dot{q}_{d,i-1}, \tag{7.2}$$

$$q_{\text{ref}}(t_i) = q_{d,i}, \tag{7.3}$$

$$\dot{q}_{\text{ref}}(t_i) = \dot{q}_{d,i}, \tag{7.4}$$

is computed by the cubic polynomial

$$q_{\text{ref}}(t) = b_0 + b_1(t - t_{i-1}) + b_2(t - t_{i-1})^2 + b_3(t - t_{i-1})^3, \qquad t_{i-1} \leq t \leq t_i, \tag{7.5}$$

where

$$b_0 = q_{d,i-1}, \tag{7.6}$$

$$b_1 = \dot{q}_{d,i-1}, \tag{7.7}$$

$$b_2 = \frac{3(q_{d,i} - q_{d,i-1}) - (2\dot{q}_{d,i-1} + \dot{q}_{d,i})(t_i - t_{i-1})}{(t_i - t_{i-1})^2}, \tag{7.8}$$

$$b_3 = \frac{2(q_{d,i} - q_{d,i-1}) + (\dot{q}_{d,i-1} + \dot{q}_{d,i})(t_i - t_{i-1})}{(t_i - t_{i-1})^3}. \tag{7.9}$$

The polynomial in (7.5) is referred to as *interpolating polynomial*. Clearly, this polynomial is twice continuously differentiable. Moreover, the trajectory obtained using this method of waypoints can easily be appended with a sequence of moves by using the end conditions of the last move as the initial condition for the subsequent move, and so on.

For this case, since the robotic arm is placed on the DDMR, the reference frame attached to the base link of the robotic arm is not necessarily inertial. Hence, we transform the position of the end-effector $p^0 \in \mathbb{R}^3$ in the base frame of reference of the robotic arm in the reference frame $\mathbb{J}(\cdot)$ of the DDMR as

$$p^{\mathbb{J}}(t) = \mathbf{R}_0^{\mathbb{J}}(t)p^0(t) + \mathbf{o}_0^{\mathbb{J}}, \tag{7.10}$$

where $\mathbf{R}_0^{\mathbb{J}} \in \mathbb{R}^{3\times3}$ captures the rotation matrix that transforms the base reference frame of

the robotic arm to the reference frame $\mathbb{J}(\cdot)$, and $\mathbf{o}_0^{\mathbb{J}} \in \mathbb{R}^3$ denotes the position of the center of the base reference frame of the robotic arm expressed in the reference frame $\mathbb{J}(\cdot)$. Similarly, (7.10) can again be transformed to the inertial frame $\mathbb{I}$ as

$$p^{\mathbb{I}}(t) = \mathbf{R}_{\mathbb{J}}^{\mathbb{I}}(t)p^{\mathbb{J}}(t) + [X_A(t) \;\; Y_A(t) \;\; Z_A(t)]^{\mathrm{T}}, \tag{7.11}$$

where $\mathbf{R}_{\mathbb{J}}^{\mathbb{I}} \in \mathbb{R}^{3\times3}$ captures the orientation of the reference frame $\mathbb{J}(\cdot)$ relative to the inertial frame $\mathbb{I}$.

7.2 Simulation results

The reference trajectories derived in Section 7.1 are given as input to the respective controllers for the DDMR and the robotic arm to generate torques to be given to the wheels of the DDMR and the arm joints of the robotic arm. The MATLAB function `ode23` was used to integrate the equations of motion 3.49, 5.38, and the adaptive laws 4.28, 6.16.

For the case of the simulation of control of the DDMR, we deduce the estimated parameters from the CAD models for a Turtlebot3. The parameters used for these simulation are provided in Appendix B.1. In order to introduce parametric uncertainties and verify the effectiveness of the proposed MRAC laws, the actual parameters were taken as multiples of the estimated parameters. Figure 7.2 shows the trajectories of the DDMR. It can be seen from Figure 7.2 that the reference trajectory follows the desired trajectory, and the actual trajectory follows the reference trajectory.

The simulated trajectory and the reference trajectory of the end-effector in the global frame are shown in Figure 7.3. In Figure 7.3, the end-effector's initial position is represented by a green dot and its final position by a red asterisk. The norm of the trajectory tracking

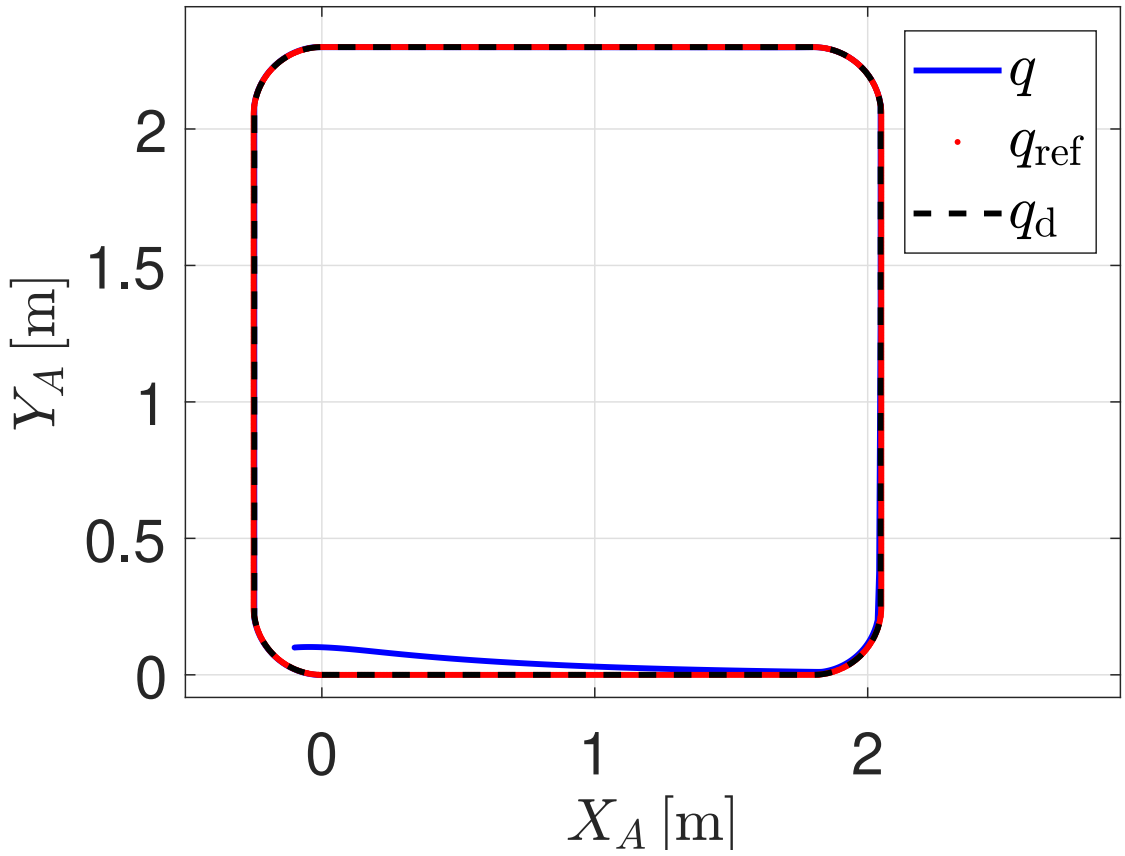

Figure 7.2: Simulation results involving a DDMR. The blue line denotes the vehicle's trajectory, the red dotted-line denotes the reference trajectory, and the black dashed-line denotes the desired trajectory.

error, that is, $\|q(t) - q_{\text{ref}}(t)\|$, $t \geq 0$, is illustrated in Figure 7.4. In these simulations, the errors in the system parameters was 90%. The parameters and the control gains are given in Appendix B.2. At $t = 8s$, the robotic arm picks a load of 2kg which is reflected in the figure. Practically, the actuators of the WidowX200 robotic arm cannot be given torques above the load torque of 3Nm.It appears from Figures 7.3 and 7.4 that, despite the parametric uncertainties and the error in the robot's initial conditions, the trajectory tracking error converges to zero.

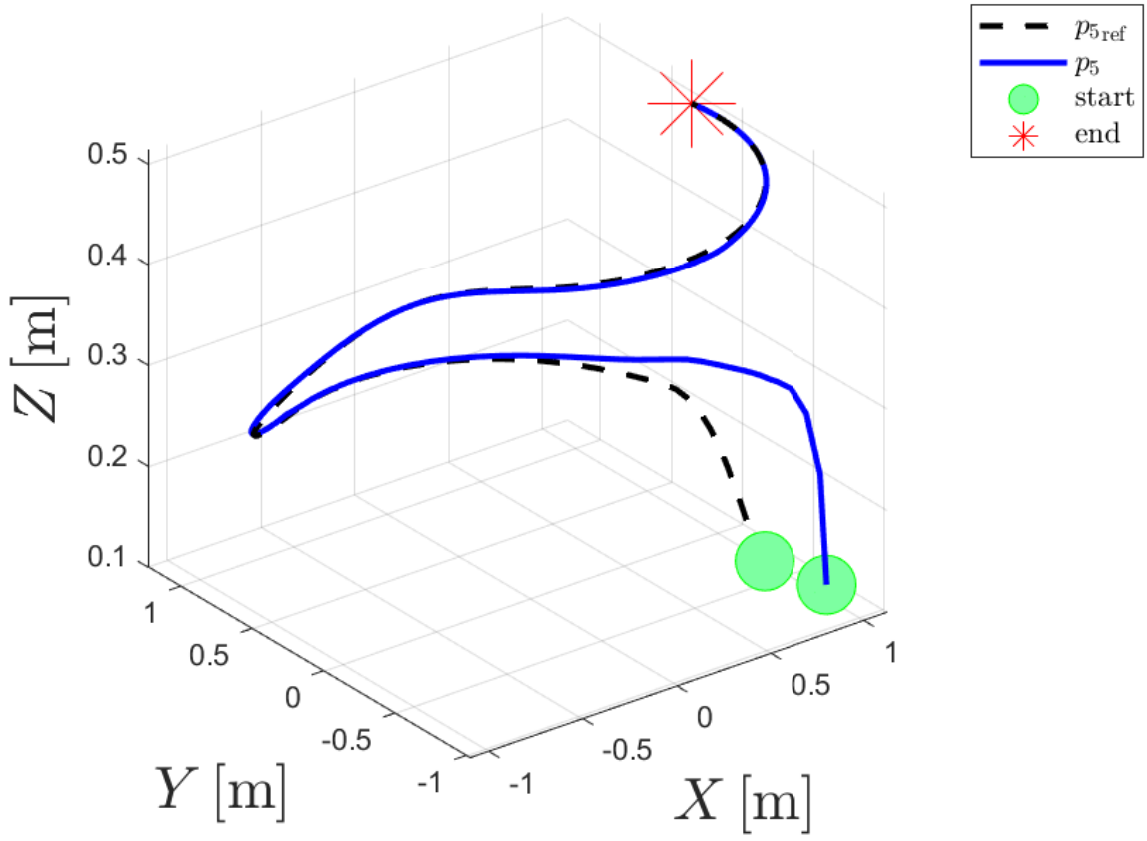

Figure 7.3: End-effector trajectory. The blue line denotes the actual simulated trajectory of the end-effector of the robotic arm and the black-dashed line denotes its reference trajectory. The end-effector's initial position is represented by a green dot and its final position by a red asterisk.

7.3 Experimental results

For the experiments, we used the TurtleBot3 as a DDMR and the WidowX 200 five-link robotic arm. For these experiments, all calculations are performed aboard the robot using an ODroid XU4 [29] single-board computer (SBC). The DDMR and the robotic arm were connected to the SBC via a USB cable to facilitate the serial communication between the computer and the motors. The TurtleBot3 uses the XM430-W210-R [30] Dynamixel motors, and WidowX 200 uses the XM430-W350-R [31] Dynamixel motors. These motors

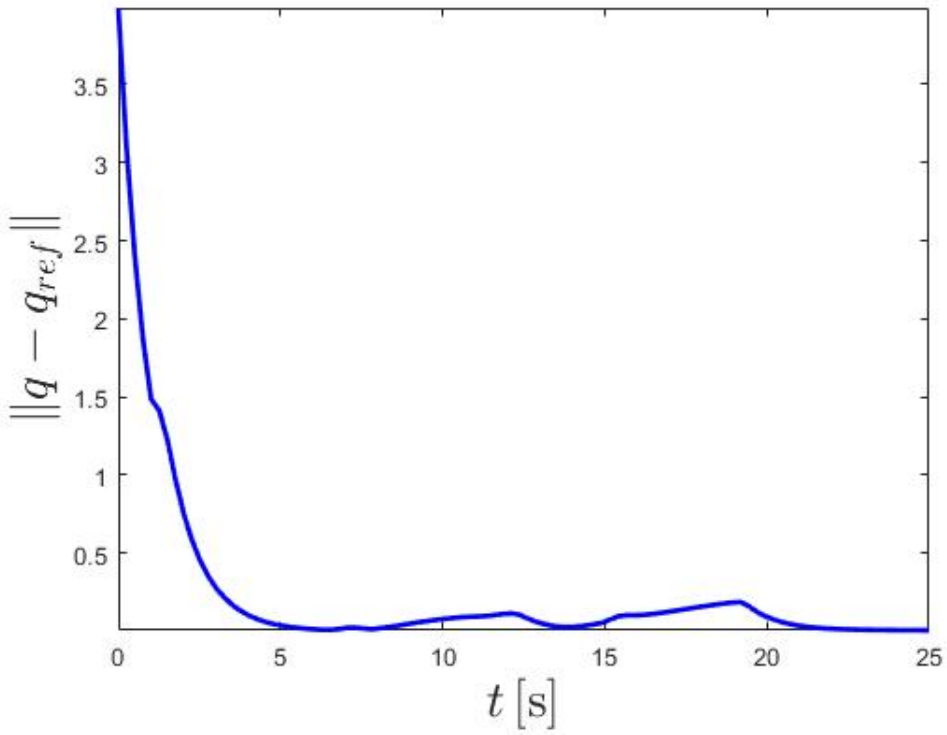

Figure 7.4: Error norm for the robotic arm trajectory.

are connected to the SBC through a USB cable with the help U2D2 power hub [32]. The Dynamixel SDK [33] provides software functions to communicate to and fro the Dynamixel motors. For the robotic arm and the DDMR, the position and velocity data can be accessed with the help of appropriate functions in the Dynamixel SDK. A Vicon motion capture system was employed to obtain the position data of the DDMR and its yaw angle. This architecture is schematically illustrated in Figure 7.5. The experimental setup with the DDMR (TurtleBot3) with the robotic arm (WidowX 200) installed on top can be seen in Figure 1.1.

The experimental results for the DDMR tracking a C-shaped trajectory and a straight trajectory are shown in Figure 7.6 and Figure 7.7. For the robotic arm, we cannot control the control the gripper link motor with current control mode. Hence, the experimental results for

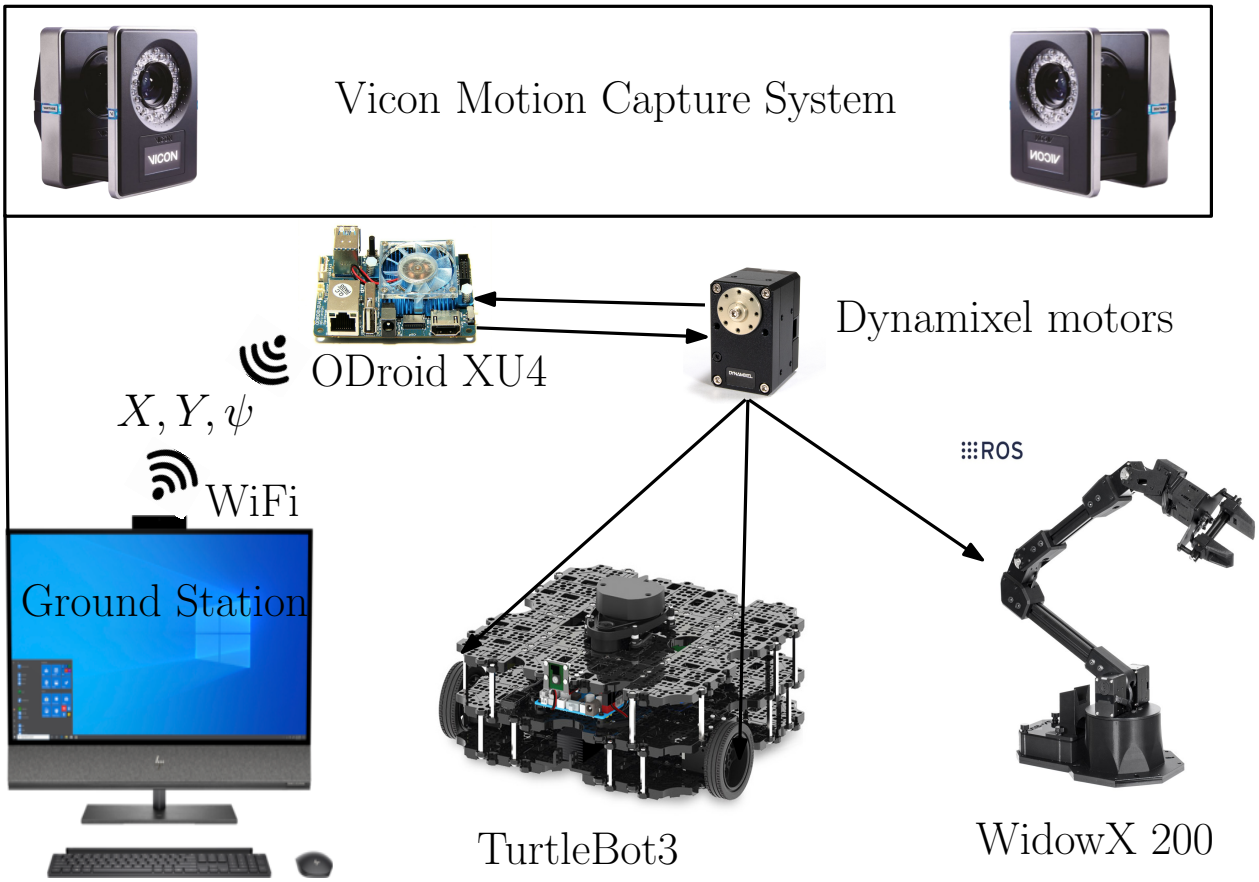

Figure 7.5: Communication diagram

the robotic arm trajectory in joint space for its four links are illustrated in Figures 7.8–7.11

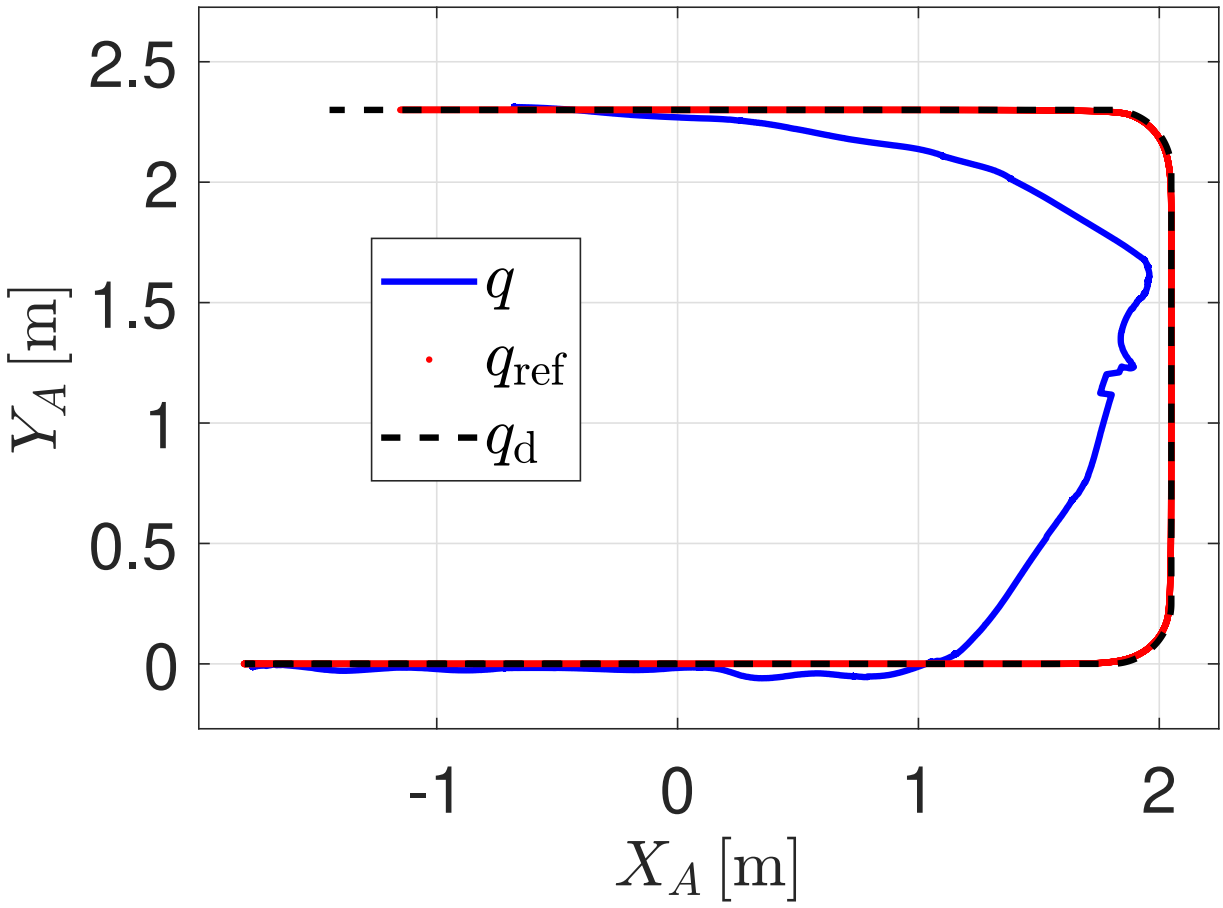

Figure 7.6: DDMR C-shaped trajectory. The blue line denotes the vehicle's trajectory, the red dotted-line denotes the reference trajectory, and the black dashed-line denotes the desired trajectory.

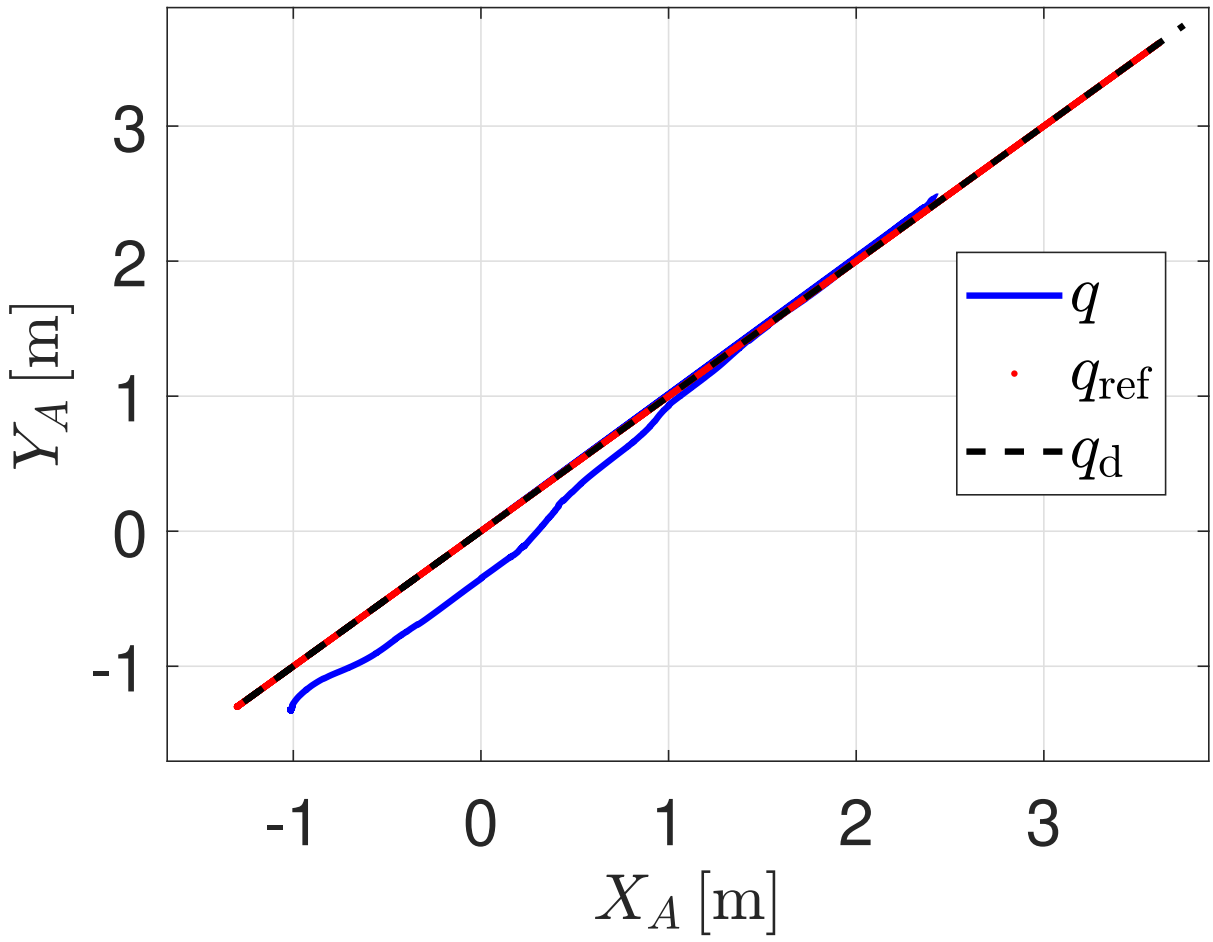

Figure 7.7: DDMR straight trajectory. The blue line denotes the vehicle's trajectory, the red dotted-line denotes the reference trajectory, and the black dashed-line denotes the desired trajectory.

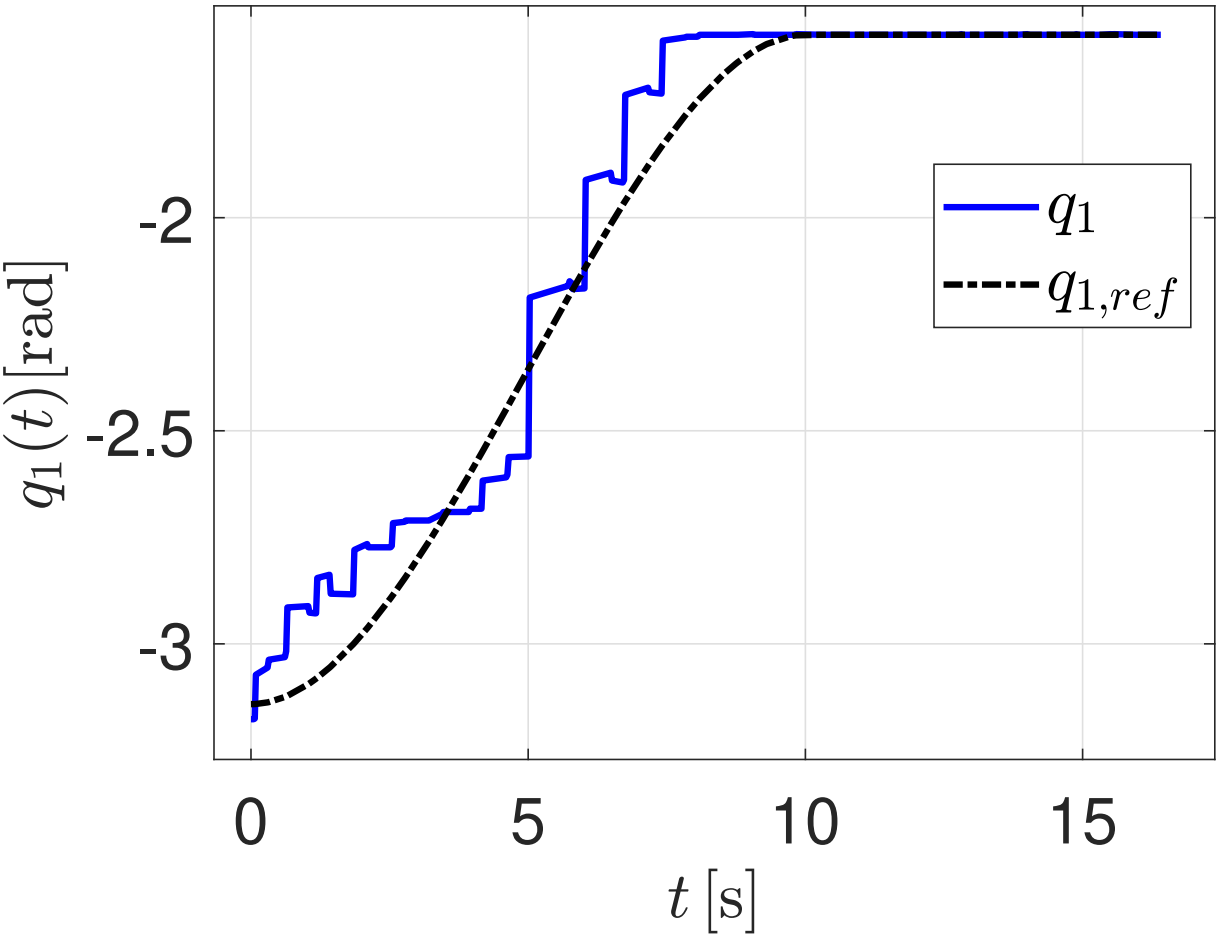

Figure 7.8: Robotic arm base link trajectory. The blue line denotes the actual trajectory and the black-dashed line denotes its reference trajectory.

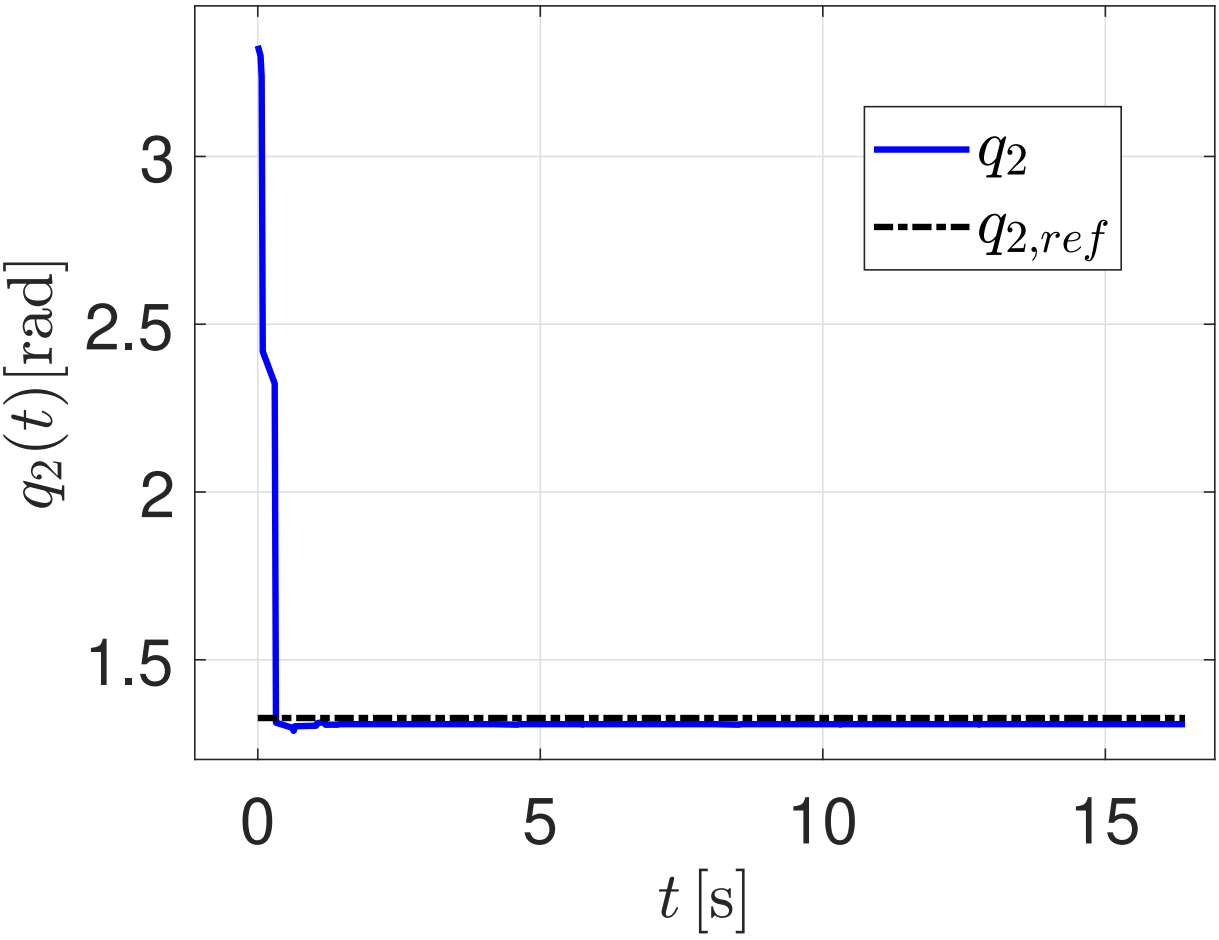

Figure 7.9: Robotic arm shoulder link trajectory. The blue line denotes the actual trajectory and the black-dashed line denotes its reference trajectory.

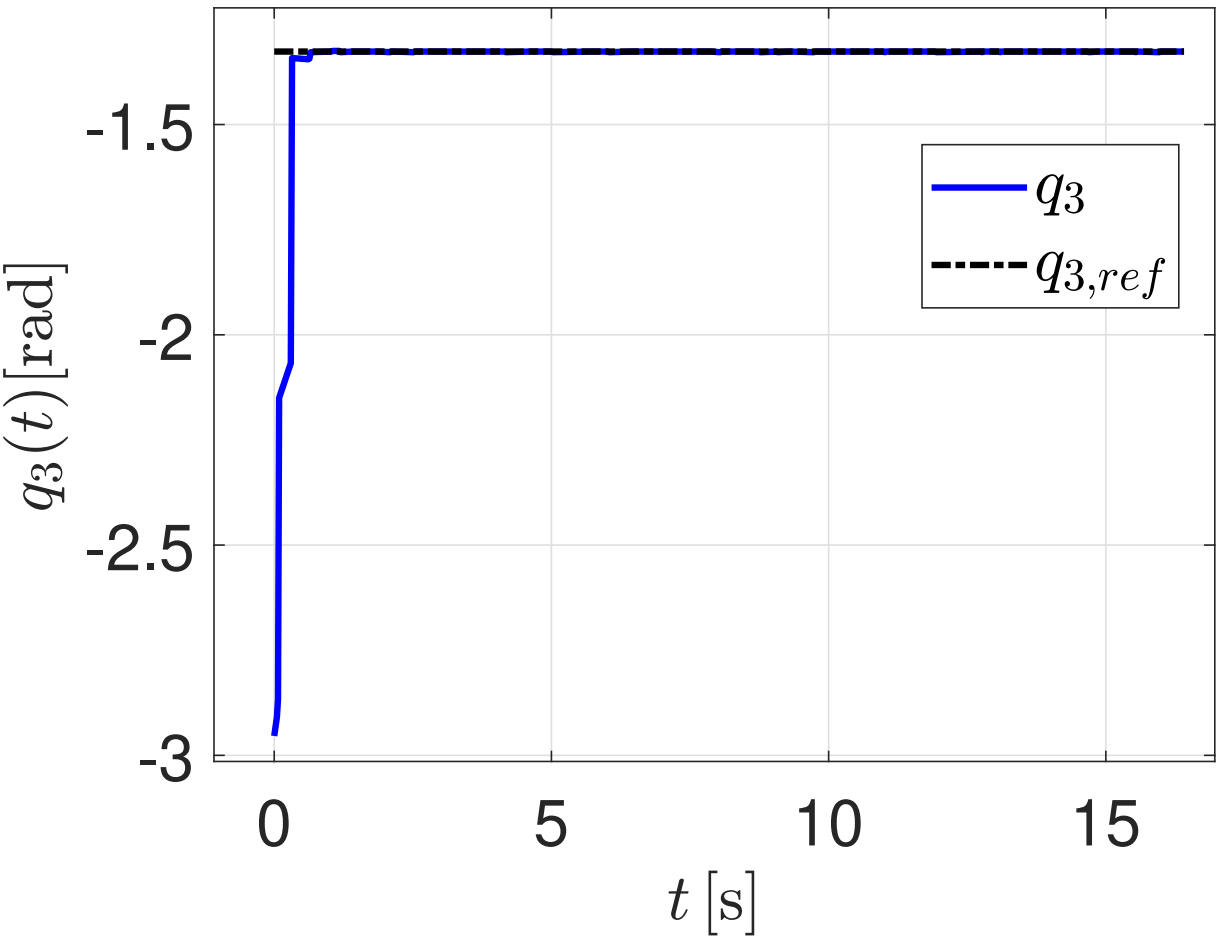

Figure 7.10: Robotic arm forearm link trajectory. The blue line denotes the actual trajectory and the black-dashed line denotes its reference trajectory.

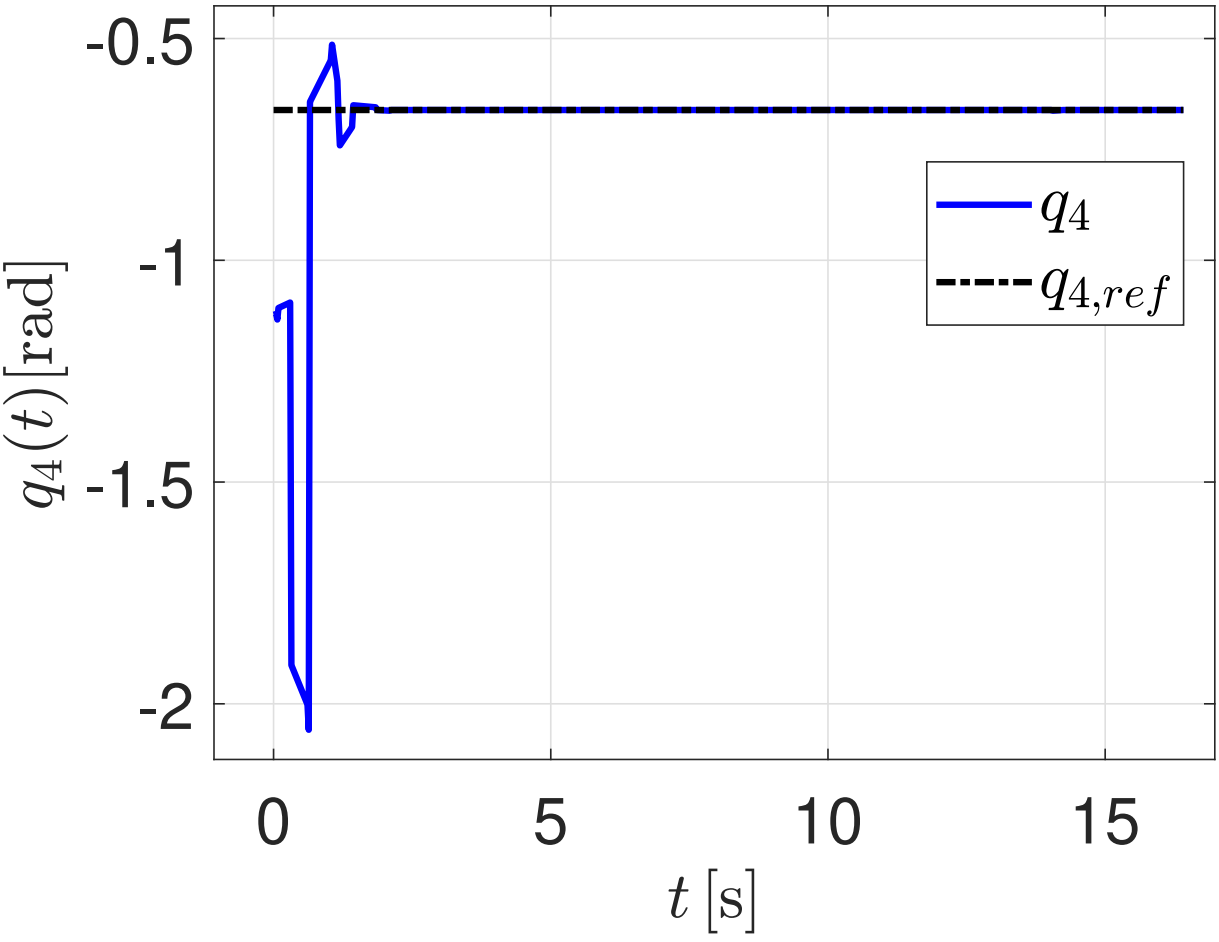

Figure 7.11: Robotic arm wrist link trajectory. The blue line denotes the actual trajectory and the black-dashed line denotes its reference trajectory.

Chapter 8

Conclusion and future work

The aim of the thesis was to implement MRAC law on a robotic system of comprising a DDMR and a robotic arm. In this thesis, we studied the dynamics of the DDMR and the robotic arm, and derived the equations of motion. Thus, we employed these dynamical models to design the MRAC for the mobile manipulator. The controller design for the DDMR and the robotic arm were validated through simulations performed in MATLAB. In these simulations, we assumed that there is pure rolling at wheels of the DDMR and the motors of the DDMR and the robotic arm are ideal, with no friction, and there is perfect torque transfer between the motor shaft and the attached link. We also assumed that the actuators are robust and can output any desired torque in order to meet the controller requirements. In practice, these assumptions are not necessarily verified. This is evident from the experimental results in Section 7.3. Indeed, the DDMR actuators can output a maximum torque of 2.06Nm. This limits the performance of the adaptive control since it may not be possible to attain a certain speed to follow a given trajectory without going beyond this saturation limit. Moreover, there is slipping at the wheels of the DDMR, which strains the controller. The tuning gains used in the simulations varied from the actual gain values used employed in the experiments.

We were able to validate the theoretical results presented in this thesis by means of actual tests on a Turtlebot3 equipped with a WidowX200 robotic arm. We performed the experiments to make the DDMR follow a line and a C-shaped trajectory, while the robotic

arm followed a reference trajectory obtained by interpolating user-defined waypoints.

For future work, improved dynamical models need to be considered for the DDMR to account for the slipping at the wheels. Additionally, the DDMR controller is presently designed only for the planar case, and future work consists in extending this framework for the non-planar dynamical model. For the case of DDMR climbing up a slope or driving down, the traction forces will affect the dynamics of the DDMR, and thus, the consideration of slipping at the wheels would facilitate controller design for the non-planar case. The present DDMR experiences slipping, and the mass of the robotic arm is 2.6 times that of the DDMR which strains the controller. Due to sudden jerks in the motion of the robotic arm, the DDMR sometimes loses contact with the ground which violates the assumptions in the dynamical model. To avoid this, the present controller can also be implemented on other robots of the same type, that is, a two-wheeled DDMR and a 5 DOF robotic arm, which are robust enough to hold the given assumptions, and with actuators with wider operating range. Next, we could consider a coupled model for the mobile manipulator. In this case, there will be synchronization in the motions of the robotic arm and the DDMR. Consider a situation in which the DDMR experiences slipping, which might cause delay in reaching the goal position at a particular moment. A coupled dynamical model would help adjust the motion of the robotic arm accordingly so that the configuration of the arm required at that particular goal position is achieved irrespective of the delay caused due to slipping.

Bibliography

[1] H. Intelligrated, "The Business Case for Robotics in Distribution Centers; market forces and new technologies give automated DCs the edge," 2020.

[2] F. Fahimi, *Autonomous Robots Modeling, Path Planning, and Control*. Alberta, Canada: Springer, 2009.

[3] R. Dhaouadi and A. A. Hatab, "Dynamic modelling of differential-drive mobile robots using lagrange and newton-euler methodologies: A unified framework." *Adv Robot Autom*, vol. 2, no. 2, 2013.

[4] L. Fan, Y. Zhang, and S. Zhang, "Dynamic trajectory tracking control of mobile robot." *International Conference on Information Science and Control Engineering*, 2018.

[5] A. Awatef and B. H. Mouna, "Dynamic modeling and inverse dynamic control of mobile robot," in *International Conference on Green Energy Conversion Systems (GECS)*, 2017, pp. 1–5.

[6] A. Mallem, S. Nourredine, and W. Benaziza, "Mobile robot trajectory tracking using PID fast terminal sliding mode inverse dynamic control," in *International Conference on Control Engineering Information Technology (CEIT)*, 2016, pp. 1–6.

[7] W. E.Dixon, D. M.Dawson, E. Zergeroglu, and A. Behal, *Nonlinear Control of Wheeled Mobile Robots*. London, Great Britain: Springer Verlag, 2001.

[8] S. Elferik and I. H. Imran, "Control of nonholonomic mobile robot based on immersion and invariance adaptive control," in *International Multi-Conference on Systems, Signals Devices (SSD15)*, 2015, pp. 1–5.

[9] Y. Tian and N. Sarkar, "Control of a mobile robot subject to wheel slip," in *J Intell Robot Sys*, 2011.

[10] Germann, Wurtenberger, and Daiss, "Monitoring of the friction coefficient between tyre and road surface," in *Proceedings of IEEE International Conference on Control and Applications*, 1994, pp. 613–618 vol.1.

[11] E.Bakker, L. Nyborg, and H. Pacejka, "Tire modeling for the use of the vehicle dynamics studies." in *SAE Technical Paper 870421*, 1987.

[12] S. Drakunov, U. Ozguner, P. Dix, and B. Ashrafi, "ABS control using optimum search via sliding modes," in *Proceedings of IEEE Conference on Decision and Control*, vol. 1, 1994, pp. 466–471 vol.1.

[13] M. W. Spong, S. Hutchinson, and M. Vidyasagar, *Robot Modeling and Control*. US: John Wiley & Sons, Inc, 2006.

[14] S. A. Ajwad, R. U. Islam, M. R. Azam, M. I. Ullah, and J. Iqbal, "Sliding mode control of rigid-link anthropomorphic robotic arm," in *International Conference on Robotics and Artificial Intelligence (ICRAI)*, 2016, pp. 75–80.

[15] T.-H. S. Li, P.-H. Kuo, Y.-F. Ho, and G.-H. Liou, "Intelligent control strategy for robotic arm by using adaptive inertia weight and acceleration coefficients particle swarm optimization," *IEEE Access*, vol. 7, pp. 126 929–126 940, 2019.

[16] K. Belda and O. Rovný, "Predictive control of 5 DOF robot arm of autonomous mobile robotic system motion control employing mathematical model of the robot arm dynamics," in *International Conference on Process Control (PC)*, 2017, pp. 339–344.

[17] M. Cholewinski and A. Mazur, "Path tracking by the nonholonomic mobile manipu-

lator," in *International Workshop on Robot Motion and Control (RoMoCo)*, 2019, pp. 203–208.

[18] Y.-X. Wu, Y. Feng, and Y.-M. Hu, "Dynamical adaptive sliding mode output tracking control of mobile manipulators," in *International Conference on Machine Learning and Cybernetics*, vol. 2, 2005, pp. 731–736 Vol. 2.

[19] Z. Li, Y. Yang, and J. Li, "Adaptive motion/force control of mobile under-actuated manipulators with dynamics uncertainties by dynamic coupling and output feedback," *IEEE Transactions on Control Systems Technology*, vol. 18, no. 5, pp. 1068–1079, 2010.

[20] S. S. Mathew and V. Jisha, "Tracking control of a mobile manipulator with external torque disturbances using computed torque control," in *2020 IEEE 17th India Council International Conference (INDICON)*, 2020, pp. 1–7.

[21] B. Chi-wu and X. Ke-fei, "Robust control of mobile manipulator service robot using torque compensation," in *2009 International Conference on Information Technology and Computer Science*, vol. 2, 2009, pp. 69–72.

[22] A. L'Afflitto, *A Mathematical Perspective on Flight Dynamics and Control* . London: U.K.: Springer, 2017.

[23] "atan2, wikipedia." [Online]. Available: https://en.wikipedia.org/wiki/Atan2l

[24] Z. Qu, *Cooperative Control of Dynamical Systems*, ser. Applications to Autonomous Vehicles. London, UK: Springer-Verlag London Limited, 2009.

[25] Y. Kanayama, Y. Kimura, F. Miyazaki, and T. Noguchi, "A stable tracking control method for a non-holonomic mobile robot," in *Proceedings IROS '91:IEEE/RSJ International Workshop on Intelligent Robots and Systems '91*, 1991, pp. 1236–1241 vol.3.

[26] Y. Liyong and X. Wei, "An adaptive tracking method for non-holonomic wheeled mobile robots," in *2007 Chinese Control Conference*, 2007, pp. 801–805.

[27] X. Shen and W. Shi, "Adaptive trajectory tracking control of wheeled mobile robot," in *2019 Chinese Control And Decision Conference (CCDC)*, 2019, pp. 5161–5165.

[28] H. Khalil, *Nonlinear Systems*, 3rd ed. Upper Saddle River, NJ: Prentice-Hall, 2002.

[29] "Odroid xu4." [Online]. Available: https://en.wikipedia.org/wiki/Atan2lhttps://www.hardkernel.com/shop/odroid-xu4-special-price/

[30] "Xm430-w210-r." [Online]. Available: https://emanual.robotis.com/docs/en/dxl/x/xm430-w210/

[31] "Xm430-w350-r." [Online]. Available: https://emanual.robotis.com/docs/en/dxl/x/xm430-w350/

[32] "U2d2." [Online]. Available: https://www.robotis.us/u2d2/

[33] "Dynamixel sdk." [Online]. Available: https://emanual.robotis.com/docs/en/software/dynamixel/dynamixel_sdk/overview/

[34] "Turtlebot." [Online]. Available: https://emanual.robotis.com/docs/en/platform/turtlebot3/overview/

Appendices

Appendix A

First Appendix

A.1 WidowX 200 robot arm

The robotic arm used in this research is the five degree of freedom serial link manipulator, WidowX 200 from Trossen Robotics. It offers a full 360 degree of rotation with 7 actuators and has a reach of 550 mm.

Figure A.1: WidowX 200 robotic arm.

A.2 TurtleBot3

The DDMR used in this research is the TurtleBot3 Waffle Pi [34]. It can attain a maximum speed of 0.26 m/s and maximum rotational speed of 1.82 rad/s. The maximum payload capacity is 30 kg.

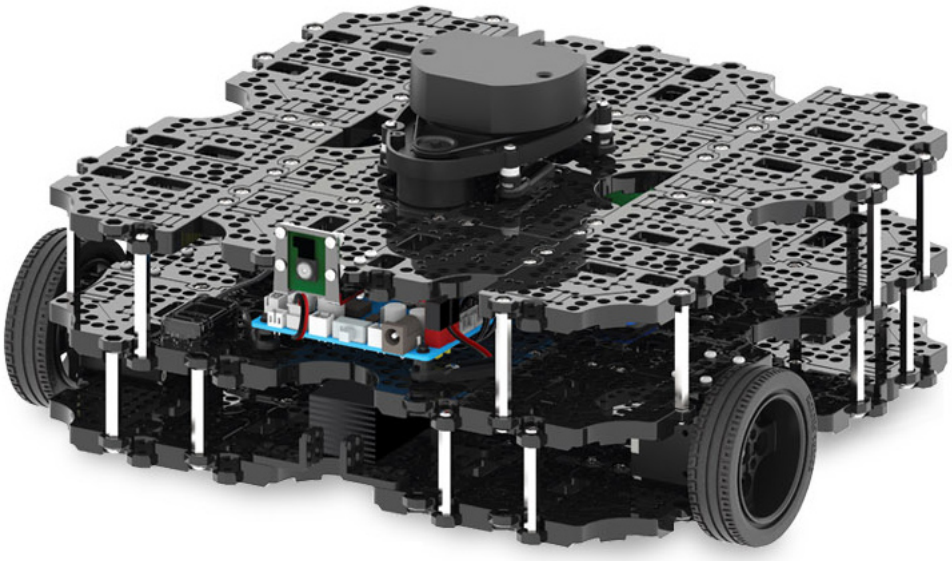

Figure A.2: TurtleBot3 Waffle Pi

Appendix B

System parameters

B.1 DDMR system parameters

The estimated system parameters for the control law computation of the DDMR (the TurtleBot) are as follows

$$\hat{m}_{\mathrm{b}} = 1.6\ kg, \tag{B.1}$$

$$\hat{m}_{\mathrm{w}} = 0.1\ kg, \tag{B.2}$$

$$\hat{I}_{\mathrm{b}} = \begin{bmatrix} 0.011184772413793 & 0 & 0 \\ 0 & 0.009844634482759 & 0 \\ 0 & 0 & 0.017740700689655 \end{bmatrix} kg/m^2, \tag{B.3}$$

$$\hat{I}_{\mathrm{w}} = \begin{bmatrix} 0.00005698 & 0 & 0 \\ 0 & 0.00006362 & 0 \\ 0 & 0 & 0.00007180 \end{bmatrix} kg/m^2, \tag{B.4}$$

$$\hat{x}_C = -0.016\ m, \tag{B.5}$$

$$\hat{y}_C = 0\ m, \tag{B.6}$$

$$\hat{z}_C = 0.008501680\ m, \tag{B.7}$$

$$l = 0.155\ m, \tag{B.8}$$

$$r = 0.033\ m, \tag{B.9}$$

$$w = 0.1435\ m. \tag{B.10}$$

and the gain matrices are

$$K_0 = 0.1\mathbb{1}_2, \tag{B.11}$$

$$K_1 = 0.1\mathbb{1}_2, \tag{B.12}$$

$$\Gamma = 0.1\mathbb{1}_4, \tag{B.13}$$

$$K_P = 4\mathbb{1}_5, \tag{B.14}$$

$$K_D = 3\mathbb{1}_5. \tag{B.15}$$

B.2 Robotic arm system parameters

The estimated system parameters for the control law computation of the robotic arm are as follows

$$\hat{m}_1 = 1.607196\ kg, \tag{B.16}$$

$$\hat{m}_2 = 0.715452\ kg, \tag{B.17}$$

$$\hat{m}_3 = 0.669306\ kg, \tag{B.18}$$

$$\hat{m}_4 = 0.416434\ kg, \tag{B.19}$$

$$\hat{m}_5 = 0.730841\ kg, \tag{B.20}$$

$$\hat{l}_1 = 0.11325\ m, \tag{B.21}$$

$$\hat{l}_2 = 0.20616\ m, \tag{B.22}$$

$$\hat{l}_3 = 0.2\ m, \tag{B.23}$$

$$\hat{l}_4 = 0.065\ m, \tag{B.24}$$

$$\hat{l}_5 = 0.131\ m, \tag{B.25}$$

$$\hat{l}_{c1} = 0.047\ m, \tag{B.26}$$

$$\hat{l}_{c2} = 0.1353\ m, \tag{B.27}$$

$$\hat{l}_{c3} = 0.118\ m, \tag{B.28}$$

$$\hat{l}_{c4} = 0.0444\ m, \tag{B.29}$$

$$\hat{l}_{c5} = 0.0955\ m, \tag{B.30}$$

$$\hat{I}_1 = 0.002175\ kg/m^2, \tag{B.31}$$

$$\hat{I}_2 = 0.00401991\ kg/m^2, \tag{B.32}$$

$$\hat{I}_3 = 0.00258893\ kg/m^2, \tag{B.33}$$

$$\hat{I}_4 = 0.00013472\ kg/m^2, \tag{B.34}$$

$$\hat{I}_5 = 0.00029738\ kg/m^2, \tag{B.35}$$

and the gain matrices are

$$K_0 = 0.01\mathbb{1}_5, \tag{B.36}$$

$$K_1 = 10\mathbb{1}_5, \tag{B.37}$$

$$\Gamma = 0.1\mathbb{1}_{14}, \tag{B.38}$$

Appendix C

Alternate linearity of parameters realization

In the control of the DDMR as well as that of the robotic arm, we have used the property of linearity of parameters. As written in (6.10), we can write the equations of motion for a mechanical system in general as

$$\mathcal{M}(q)a + \mathcal{C}(q,\dot{q})v + \mathcal{K}(q) = \mathcal{Y}(v,a,q,\dot{q})\Theta, \qquad (v,a,q,\dot{q}) \in \mathbb{R}^n \times \mathbb{R}^n \times \mathbb{R}^n \times \mathbb{R}^n, \qquad \text{(C.1)}$$

where $\mathcal{Y} : \mathbb{R}^n \times \mathbb{R}^n \times \mathbb{R}^n \times \mathbb{R}^n \to \mathbb{R}^{n \times N}$ is the regressor matrix and $\Theta \in \mathbb{R}^N$ is the vector of parameters.

Alternatively, we can write (C.1) as

$$\mathcal{M}(q)a + \mathcal{C}(q,\dot{q})v + \mathcal{K}(q) = \Theta^{\mathrm{T}}\Phi(v,a,q,\dot{q}), \qquad (v,a,q,\dot{q}) \in \mathbb{R}^n \times \mathbb{R}^n \times \mathbb{R}^n \times \mathbb{R}^n, \qquad \text{(C.2)}$$

where $\Phi : \mathbb{R}^n \times \mathbb{R}^n \times \mathbb{R}^n \times \mathbb{R}^n \to \mathbb{R}^N$ is the regressor vector and $\Theta \in \mathbb{R}^{N \times n}$ is the matrix of parameters.